Geochemical Processes of Trace Metals in Fresh–Saline Water Interfaces. The Cases of Louros and Acheloos Estuaries

Michael Scoullos and Fotini Botsou

Abstract Fresh–saline water interfaces are sites of major transformations on the speciation and the distribution of trace metals, through complex processes. The present chapter considers trace metal geochemical processes at fresh–saline water interfaces of representative Greek riverine systems, namely of those of the perennial medium-sized Louros River and the big and highly fragmented Acheloos River. Dissolved and particulate metals, as well as metal fractions in the sediments, are considered in combination with physicochemical parameters, and mineral magnetic measurements are used for tracing the origin of particle populations (lithogenic, anthropogenic, authigenic), and their compositional alterations during their passage from the rivers, through the interfaces, to sea. The interfaces of the two systems have distinct characteristics both on a spatial and a temporal scale, thus allowing for a diversity of trace metal behaviour patterns to emerge. In the small, perennial Louros system, trace metals are trapped within the thin, yet stable salt wedge. In the heavily fragmented Acheloos system, variations of the water and sediment discharges have moved the active interface landwards, where due to the reduction of dilution effects by inert, detrital particles, the fingerprint of the authigenic and anthropogenic component of trace metals has become more pronounced. The results of the research carried out in the two distinctive fresh–saline water interface systems are important not only in order to enlighten us about the geochemical processes in nature, but also in order to provide the necessary knowledge to properly manage these systems for the benefit of the environment and the sustainable development of the impacted areas.

Keywords Distribution coefficient, Estuarine mixing, Salt wedge, Sorption–desorption processes, Trace metals

M. Scoullos (✉) and F. Botsou
Laboratory of Environmental Chemistry, Department of Chemistry, National and Kapodistrian University of Athens, Panepistimioupolis Zografou, 157 84 Athens, Greece
e-mail: scoullos@chem.uoa.gr

Contents

1   Introduction

Fresh–saline water interfaces, including a variety of systems such as river mouths, estuaries, rías and coastal lagoons, are recipients of major discharges of trace metals deriving from land runoff, industrial and urban discharges and atmospheric precipitates (e.g. [1–3]). The aforementioned systems are characterised as "chemical reactors" wherein, under strong hydrodynamic and physicochemical gradients, complex heterogeneous processes greatly affect the distribution of trace metals, and eventually, the fluxes of metals that reach the adjacent sea [4–7].

The geochemical dynamics of fresh–saline water interfaces is influenced by the specific, physical and climatic conditions that control the discharge rates and the residence time of trace metals, the geomorphological conditions that affect the overall structure of these systems, and the numerous and complex biogeochemical processes that define the distribution of trace metals over the particulate and dissolved phase, thus the composition of the deposited sediment. The biogeochemical processes include complexation reactions with dissolved organic and inorganic ligands, adsorption/desorption reactions onto inorganic and organic suspended particles, flocculation and coagulation of colloidal and particulate species and remobilisation from sediments. All these processes vary, depending on pH, ionic strength, the amount and the composition of suspended particles, as well as with redox conditions [5, 8, 9].

The changes in the distribution between the dissolved and the particulate phase are demonstrated through the addition, or the removal of dissolved trace metals (e.g. [4, 6, 7]). Sediments in such transitional systems can act in some cases as sinks, and in some other cases as secondary sources of metals for the adjacent marine environment. The character of their specific function is defined by complex physical, geochemical and biological factors [10–12] and might change periodically.

In the riverine fresh–saline water interfaces perhaps the most significant physical factor is the energy of the overlying flow. Strongly dependent on the flow, both in terms of volume and velocities, are the residence time of waters and suspended particulate matter at the fresh–saline water interfaces [13]. In the stratified estuary of the big Rhone River (drainage basin: 98,800 km^2) with an average water discharge of 1,700 m^3/s that reaches more than 8,000 m^3/s at flood events [2], the

rapid flushing of the water and a large fraction of particulate matter in the brackish surface plume (in a matter of a few days) reduces the quantity of suspended matter available for exchanges between the dissolved and particulate phase, as well as the contact time between the particles and the solution. In this case, dilution effects predominate over adsorption/desorption processes [14]. Of course, besides the kinetic control (rates of chemical reactions in relation to estuarine size and hence freshwater retention time) thermodynamic considerations are also important: re-suspension of sediments driven by strong tidal currents or even wind stress, and landward movement of suspended particles depleted in adsorbed metals, or in situ addition of particles of biogenic origin, could generate disequilibrium with respect to particle-water metal exchanges, thus enhancing solution–particle interactions, even in small estuarine systems [13, 15, 16].

Other factors interlinked to the prevailing hydrological regime are the dilution effects (e.g. [2, 17]), changing of the redox status of waters and/or sediments (e.g. [5, 18]) and benthic fluxes [4, 19], re-suspension of sediments [20], as well as the granulometry and the composition of suspended particulate matter (SPM) (e.g. [21]). The particle size distribution and the composition of SPM (i.e. organic, inorganic, inert minerals and highly reactive Fe/Mn oxyhydroxides, complex surfaces or flocculated aggregate constituents) are fundamental properties for the reactivity of trace metals during estuarine mixing, settling velocities and re-suspension potential within the mixing zone, and dispersion pathways beyond the mixing zone [3, 16, 17, 22].

In the Mediterranean basin, apart from a few large, perennial rivers, with catchment areas larger than 20,000 km^2, such as the Rhone, the Ebro (Spain), the Nile, the Evros (Greece) and Po, there are hundreds of medium (<5,000 km^2) and small (<500 km^2) streams, many of which are intermittent or ephemeral, representing ~12% of the Mediterranean's drainage basin. This figure rises up to ~42.5% if the Nile river basin is excluded [23]. In the medium/small rivers, the low river flow and the absence of strong tidal currents result in the suppression of the mixing zone to only a few kilometers, in contrast, for example, to the macrotidal large Scheldt Estuary that extents over 100 km and has a residence time of two to three months depending on the seasonal variations of the river flow [18, 19]. In these systems, river discharge, rather than marine influences, plays the dominant role on the stratification of the estuary and the advance or retreat of the salt wedge [24].

A very important feature of the river flow, particularly in the Mediterranean, is the high variability which exceeds the margins of seasonality, not only because of water scarcity linked to the semi-arid character of the region and other natural phenomena (e.g. the enhanced frequency of droughts and floods attributed to climate change), but also due to severe anthropogenic interventions, such as dams, water abstraction and flow diversions. These changes have a direct impact on water and sediment flows and result in a series of complex indirect implications on the behaviour of trace metals. For example, the reduction of the Strymon River inflows into the N. Aegean Sea, by approximately 30% due to extensive irrigation

and reduced precipitation, favoured the development of a salt wedge intruding the upper part of the estuary [24].

Due to the unique combination of the physical, geomorphological and biogeochemical factors in each system, there is no common pattern of trace metals behaviour in fresh–saline water interfaces. Thus, despite the wealth of literature reports for the better understanding of the geochemical dynamics and processes in estuarine systems, further research on their structure and on the distributions of trace metals in their waters and sediments is still needed.

The present chapter elaborates on a number of important aspects of trace metal transport from land to the sea and the transformations occurring at the fresh–saline water interfaces that emerged from the examination of specific cases studied in the Laboratory of Environmental Chemistry (LEC) of the University of Athens, Greece, under the supervision of the first author who also introduced Chemical Oceanography to Greece in the late 1970s. Since then, multiple projects have been carried out by LEC scientists, in many active fresh/saline water interface systems ([25–31]), and valuable insights on the behaviour of trace metals in these systems have been gained.

The present work focuses on two riverine systems, namely those of rivers Louros and Acheloos, relying to a large extent on the work published by Scoullos et al. [28] and Dassenakis et al. [25, 32], respectively. These systems have very distinct characteristics with respect to their flows and sediment discharges, the interventions along their river courses, as well as the activities hosted in the respective catchment areas. The conditions of formation, as well as the surface of the fresh–saline water interface, vary widely among the systems primarily due to the diversity in their geomorphological features and hydrological regimes. In the present review, the selected systems demonstrate the diversity of patterns of trace metal behaviour and the conclusions drawn can be readily applicable to numerous comparable systems of the Mediterranean coastline and beyond.

2 Description of the Systems

The drainage basins of the Louros and Acheloos Rivers occupy an area of 785 km^2 [33] and 6,478 km^2 [34], respectively. Mediterranean and Black Sea rivers that drain catchments of <5,000 km^2 are considered as small/medium rivers [23], hence the two rivers are considered as representative examples of large (Acheloos River) and medium/small (Louros) Mediterranean systems. Both river basins are located in the wet, western part of the country and receive annually 808 mm (Acheloos) and 925 mm (Louros) of precipitation [33, 34].

The Louros River discharges into the semi-enclosed Amvrakikos Gulf (Fig. 1), which is connected through a narrow, silled, natural channel to the Ionian Sea. The Amvrakikos wetland, consisting of the Louros and Arachthos deltas and several lagoons, is one of the most important protected wetlands of Europe, designated under the Ramsar Convention and the European Communities' Legislation.
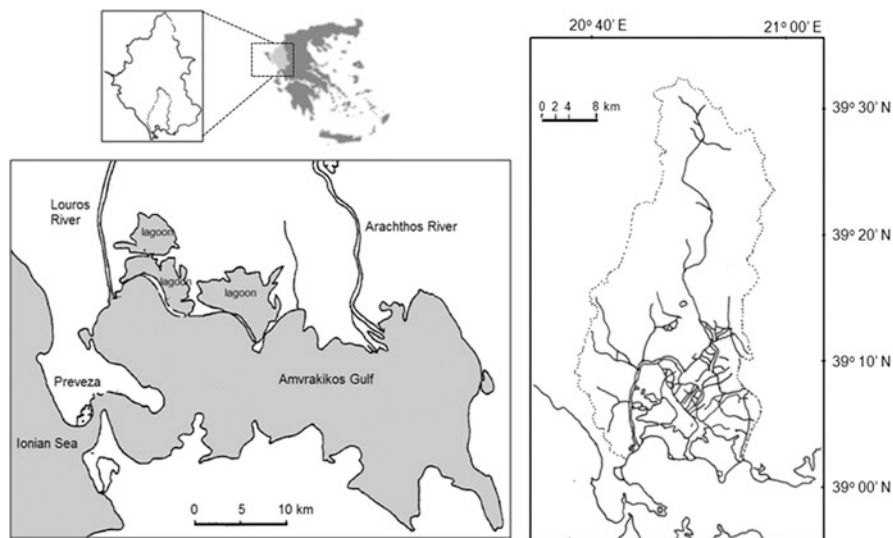
Fig. 1 The Louros watershed (marked with *dotted line*) and its estuary in the Amvrakikos Gulf. Note the dense network of artificial channels in the lower reaches of the watershed (*right panel*)

The Louros River has a length of approximately 80 km, an average width of 12 m, a depth of approximately 4.5 m and its mouth is silled by a very shallow bar of 0.6 m depth [28]. It has an average flow of 19 m^3/s [33]; however, extensive water abstraction for irrigation results in the decline of river runoff, particularly during the low flow season [28]. The drainage basin consists mainly of carbonate rocks (66%) and clastic (flusch and alluvial) sediments, resulting in relatively low sediment fluxes (0.8 × 10^6 t; [33]). Within the basin, more than 100 large and small agricultural industries are in operation [35].

The Louros Estuary provides insights onto the "microstructure" of a typical salt wedge system of low river flow and negligible tidal range. The highest stratification occurs during the summer months, when a deep pycnocline with considerable density gradients separates the fresh and saline water layers. During this season, saline water intrudes the estuary near the river bed, despite the existing shallow sill, and forms a thin (approximately 15 cm) salt–wedge water mass, which occupies the near-bottom layer with its thin end, pointed upstream. A detailed sampling took place during a period of minimum river runoff (10 m^3/s) and maximum penetration of saline water enhanced by southerly winds by employing a portable salinometer and a submersible micro-pump, which allowed for a thorough investigation at the fresh–saline water interface.

The second case study concerns the Acheloos River (Fig. 2), which is the second longest river in Greece (255 m). The Acheloos River is known from the Greek mythology as a river "God" fighting with Hercules over the river nymph Deianeira. The river is strongly fragmented by four large dams/hydroelectric plants located at the upper and middle part of the basin that have resulted in significant alteration of
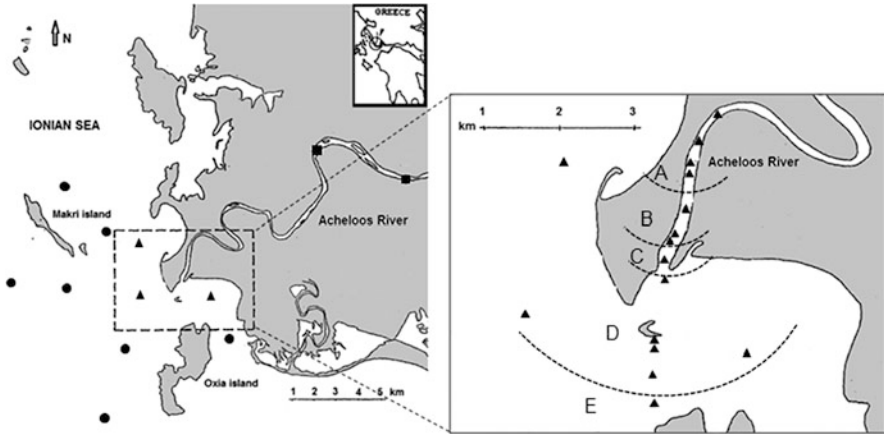
Fig. 2 The Acheloos River system (*right*), the Acheloos Estuary (*left*) and the grid of stations in the riverine (marked with *rectangles*), estuarine (marked with *triangles*) and the marine (marked with *circles*) sector of the system. *Left panel* shows the zones A–E (see text for description) of the estuarine sector

the hydrological regime as it concerns both the volume of the discharge and its seasonality: the highest maximum discharge occurs in July due to peak hydropower production. It is estimated that 30% of the annual flows occurs in short intervals during summer, compared to 11% prior to dam constructions [34]. The mean annual runoff at Kastraki (catchment area: 4,118 km^2) is 96.7 m^3/s and the range of measured monthly runoffs over the period 1980–2000 is between 13 and 1,118 m^3/s [34]. Runoff may decline further in some periods to less than 10 m^3/s, due to water abstraction for irrigation [25]. Furthermore, significant sediment retention in reservoirs (>80% of the annual sediment flux) has occurred with consequences in the sedimentation processes in the estuary.

At the river mouth there is a shallow, sand bar of 50–80 m width. The water depth at the bar area is less than 1 m, whereas upstream is approximately 4 m. The water depth increases abruptly (>40 m) at a distance of 3 km offshore [25, 32].

In the Acheloos Estuary seawater penetrates into the river bed and forms a salt wedge with significant salinity gradients between surface and bottom waters. During periods of limited freshwater supply, the fresh–saline water interface is shifted towards the upper part of the river, about 2–3 km from the river mouth. When the freshwater supply increases, the fresh–saline water interface obtains a vertical front, which lies close to the river mouth on the marine side of the bar [36]. The presence of a salt wedge of varying size and the seasonal variations of the high turbidity zone are some of the consequences of the significant river flow variations (in general reduction) due to the operations of the hydropower plants and other human interventions along the river course.

The Acheloos Estuary does not receive any direct industrial wastewater discharges from known point sources. However, it receives the land washout and agricultural discharges of a relatively large catchment area and cultivated lands

near the estuary, where agricultural land covers 41% of the area [37]. The estuary is of high environmental importance, as the discharges of the Acheloos affect not only the important Messolongi lagoons and other smaller wetlands, but also the distributions of nutrients of the entire northwestern section of the Patraikos Gulf and the nearshore part of the Ionian Sea, acting as a significant nitrogen source, attributed largely to the washout of fertilisers [36, 38].

The Acheloos River has received international attention because of the ongoing plans for its diversion towards Thessaly and the Aegean Sea, for the past 30 years. The Acheloos Water Transfer Project includes the diversion of a large portion of the Acheloos waters (today at a reduced rate of 0.6 km^3/year) towards the Pinios River basin to serve hydropower generation, drinking water supply, irrigation and improvement of the surface and groundwater quality of the intensively cultivated Thessaly plain. This project has been blocked by various sectors of the Greek society including NGOs and several decisions of the High Courts [34, 39–41].

3   Materials and Methods

Physicochemical parameters, including salinity, pH and dissolved oxygen (DO), were measured in situ by portable instruments. The water samples were collected by mini, whole-plastic submersible pumps, horizontal Hydro-Bios and Niskin bottles depending on the water depth of each station. Surface sediments were collected by means of grab samplers and short cores, and by means of a pneumatic corer [42] and Perspex tubes.

In the laboratory, water samples were filtered through 0.45 μm Millipore filters. Trace metal in the dissolved phase was pre-concentrated on a Chelex-100 resin, following a slight modification of the Riley and Taylor [43] method after Scoullos and Dassenakis [44]. Water sample handling was carried out in a clean box to prevent contamination. In the case of the Louros case study, the filters holding the particulate matter were divided into two. One half of each filter was treated with boiling conc. HNO_3 in covered PTFE beakers, whereas the other half was treated with cold 0.5 N HCl [28]. In the case of the Acheloos River, the filters were digested only with boiling conc. HNO_3. In this review, the results of analyses of $n = 128$ water samples in the case of Acheloos Estuary and $n = 17$ water samples in the case of Louros Estuary are reported. The sediment samples of both the Louros (number of sediment samples $n = 12$) and Acheloos systems ($n = 14$) were digested in a hot plate with concentrated HNO_3. The labile, non-lattice held fraction of trace metals were extracted by the single-step 0.5 N HCl method of Agemian and Chau [45]. In addition to the dilute HCl extraction, the sequential extraction scheme (SES) described in Scoullos and Oldfield [46] and summarised in Table 1 was employed in the sediment samples of the Acheloos Estuary. Trace metal concentrations were determined by means of Graphite Furnace or Flame Atomic Absorption Spectroscopy.

Table 1 Reagents and leachable fractions of metals by sequential extraction scheme after Scoullos and Oldfield [46]

Extraction step	Reagents	Duration and temperature of extraction	Fraction of metals
1	1M MgCl$_2$	16 h, room temperature	Easily exchangeable
2	1M CH$_3$COOH-NH$_2$OH·HCl	16 h, room temperature	Non-exchangeable, non-lattice held, inorganic
3	0.05M EDTA	24 h, room temperature	Organic
4	Conc. HNO$_3$: HClO$_4$ (2:1)	180°C evaporation until near dry (3 times)	Residual

In all studies, determinations of trace metal contents in sediments were performed in the <63 μm fraction in order to minimise grain-size effects [47]. As a second step, a geochemical normalisation to Al was applied, in order to reduce residual variance due to compositional (mineralogical) differences within and between the cores, despite the fact that the <63 μm fraction is considered as the least affected by grain-size effects [47, 48].

Organic carbon content was determined after the Gaudette et al. [49] method. Mineral magnetic measurements were determined by the methods and instrumentation described in Scoullos and Oldfield [46], and Scoullos, Botsou and Zeri [50].

4 Results and Discussion

4.1 *The Louros Estuary*

Physicochemical parameters (salinity, pH, Suspended Particulate Matter – SPM) allowed for the identification of three distinct water masses:

(a) The overflowing, seaward moving, riverine water mass. Salinity and pH range from 0.5 and 7.0 at the upper part of the river, respectively, to 4.2 and 7.3, respectively, at the lower reaches of the estuary.
(b) The salt water wedge, occupying the deep layer near the river bed. The salt wedge has a length of approximately 5.7 km, an average width of 15 cm, although these characteristics may fluctuate with time, depending directly or indirectly on seasonal phenomena, mainly the river runoff, the ambient temperature and the prevailing winds. The ranges of salinity and pH are 25.6–28.9 and 7.6–7.8, respectively.
(c) The marine water outside the river mouth, with typical marine water salinity (34.2–36.9) and pH values (7.8–8.2).

The aforementioned structure of the system is graphically presented in Fig. 3.

The descriptive statistics of Al, Fe and trace metals concentrations in the dissolved phase and their contents of the particulate matter (extracted by conc.
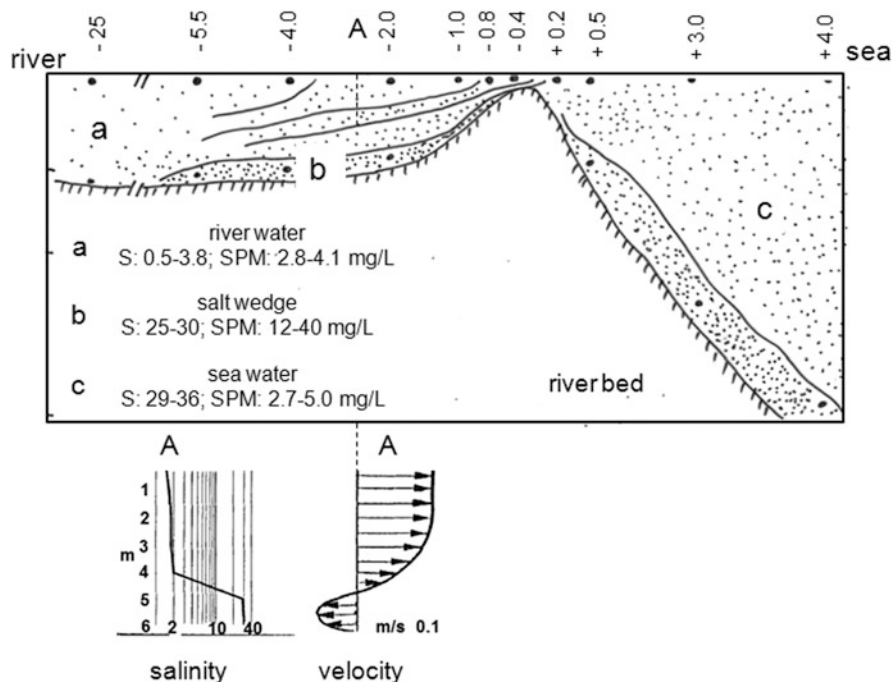
Fig. 3 Cross section of the Louros Estuary indicating the three distinct water masses: (**a**) the riverine, (**b**) the salt wedge and (**c**) the marine. Horizontal axis shows the distance of sampling stations (marked with *circles*) from the mouth of the river: (*minus*); upstream; (*plus*): offshore. Density of dots in the three water masses represents the concentration of SPM. Isohalines have been determined by in situ measurements. Velocity corresponds to average current. Modified from Scoullos et al. [28]

HNO_3) in the three masses of the system are given in Table 2. Dissolved Fe, Mn and Cu concentrations at the riverine water mass are much lower than the average concentrations of world's rivers [51], whereas dissolved Pb and Zn are slightly higher. Particulate Al and Fe are lower than the world's average values, because of the non-complete dissolution of the crystal lattice of aluminosilicate minerals by the boiling conc. HNO_3. Particulate Cu is lower, whereas particulate Mn, Pb and Zn are slightly higher than the world's average, indicating probably the influence of local or upstream anthropogenic activities.

With regard to the variations of dissolved trace metal concentrations in the three masses of the system, the data in Table 2 show that the trace metal levels in the marine water mass are similar (e.g. Pb), or even higher (e.g. Cu and Zn) than in the river water. This distribution pattern is rather unusual for most estuaries, where the adjacent seawater concentrations are normally lower. Furthermore, based on the average values, the highest concentrations of all the metals studied are found in the salt water wedge, indicating the addition of metals in solution at the salt stress interface (Table 2). Figure 4 shows the variation of dissolved trace metal

Table 2 Ranges and average (in parenthesis) concentrations of Al, Fe and trace metals in the dissolved (Diss.) and particulate (Part.) phase, as well as partition coefficient (K_D) in the three distinct water masses of the Louros system (number of samples, $n = 17$)

	Al	Fe		Mn		Cu		Ni		Pb		Zn	
	Part	Diss.	Part.	Diss.	Part.	Diss.	Part.	Diss.	Part.	Diss.	Part.	Diss.	Part.
RIV (a)	0.3–4.7 (3.8)	0.95–2.30 (1.39)	0.31–4.0 (3.0)	0.07–0.26 (0.15)	304–6,821 (5,145)	0.24–0.60 (0.38)	14.6–88.6 (58.6)	0.45–5.20 (1.60)	132–878 (454)	0.05–0.48 (0.24)	18.5–220 (71.8)	0.50–2.10 (1.33)	30.9–371 (272)
SW (b)	2.0–3.2 (2.7)	1.50–2.10 (1.83)	2.3–2.7 (2.5)	31.4–45.4 (36.4)	2,614–20,972 (10,528)	5.20–5.80 (5.43)	97.2–1,056 (524)	3.10–5.10 (4.00)	368–392 (383)	0.14–0.60 (0.30)	40–344 (166)	21.4–41.3 (28.1)	598–1,696 (1,102)
MAR (c)	0.3–2.3 (1.1)	1.00–2.00 (1.59)	0.3–1.5 (0.72)	0.08–0.46 (0.23)	391–1,471 (840)	0.40–0.85 (0.60)	19.4–59.4 (35.4)	0.90–2.40 (1.74)	111–361 (187)	0.15–0.30 (0.23)	8.2–62.5 (37.9)	0.82–2.05 (1.59)	50.8–269 (170)
ORM	1.98	2.70	1.1	0.50	500	2.20	28.6	9.20	127	0.50	29.4	2.30	50.8
World Rivers	8.7	66.0	5.81	34.0	1,679	1.48	75.9	0.80	74.5	0.08	61.1	0.60	208
K_D													
RIV (a)		6.13–7.62 (7.28)		6.07–7.98 (7.58)		4.39–5.48 (5.16)		4.40–6.20 (5.55)		4.59–6.64 (5.39)		4.31–5.81 (5.28)	
SW (b)		7.10–7.18 (7.13)		4.91–5.66 (5.33)		4.26–5.31 (4.81)		4.89–5.07 (4.99)		5.46–5.88 (5.70)		4.44–4.67 (4.58)	
MAR (c)		6.17–6.82 (6.56)		6.07–7.05 (6.54)		4.25–4.91 (4.67)		41.47–5.48 (4.89)		4.61–5.48 (5.10)		4.56–5.17 (4.95)	
ORM		6.75		6.47		4.25		4.47		4.77		4.57	
European estuaries		Not given		Not given		4.0–5.0		4.0–4.5		5.0–7.0		4.0–5.0	

Dissolved metal concentrations are expressed in μg/L. Particulate contents refer to the boiling conc. HNO_3 extractable fraction and are expressed in the (w/w) form (Al, Fe in %, trace metals in mg/kg). Data for the station which is located outside river mouth (ORM) and is affected by re-suspension are given separately. K_D is expressed in logarithmic values. For comparison we report also the average concentrations of major and trace elements in the dissolved phase and suspended sediments of World Rivers [51] and the K_D values reported in European estuarine and coastal systems, reviewed by Balls [52]
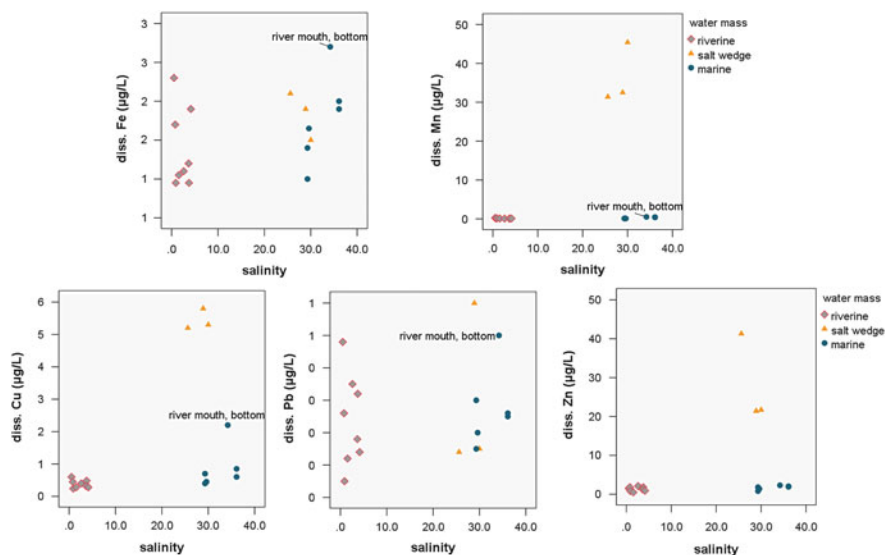
Fig. 4 Plots of dissolved trace metal concentrations against salinity in the Louros Estuary. The station outside the river mouth affected by re-suspension of sediments is marked as "river mouth, bottom"

concentrations with salinity. All metals show a non-conservative behaviour. Two different distribution patterns can be detected. The first distribution pattern is followed by Fe and Pb, for which the concentrations are highly scattered both at the low and the high salinity regime. The high variability of metal concentrations at the low salinity river water suggests the existence of local sources of these metals at the lower reaches of the river. Further downstream, the addition of dissolved metals is related to solid–solution interactions where the solid phase could be either the particulate matter, or re-suspended sediments, as in the case of the bottom water outside the river mouth (station shown in Fig. 4). Re-suspension of sediments at this station is evidenced by the high SPM concentrations, reaching 500 mg/L. The second distribution pattern is followed by Cu, Zn and Mn. In this case, the plots of dissolved metal concentrations against salinity show that addition processes clearly take place at the salt wedge.

Particulate metals (w/v), extracted by conc. HNO_3 and 0.5 N HCl, are accumulated in the salt wedge, as it becomes evident from their concentrations, which are considerably higher than those of water masses (**a**) and (**c**) (Figs. 5a–d). The enrichment of both leachable forms of metals in the salt wedge is mainly attributed to the high SPM concentrations in the water mass (**b**), with an average value (± 1 standard deviation) of 28.9 ± 14.4 mg/L, whereas in the river water it averages 8.88 ± 16.1 mg/L.

Figure 5e, g shows the variation of average values of 0.5 N HCl leachable trace metals contents (w/w) in the three masses of the system. This figure, combined with the data from Table 2 on trace metal contents of the particulate matter extracted by
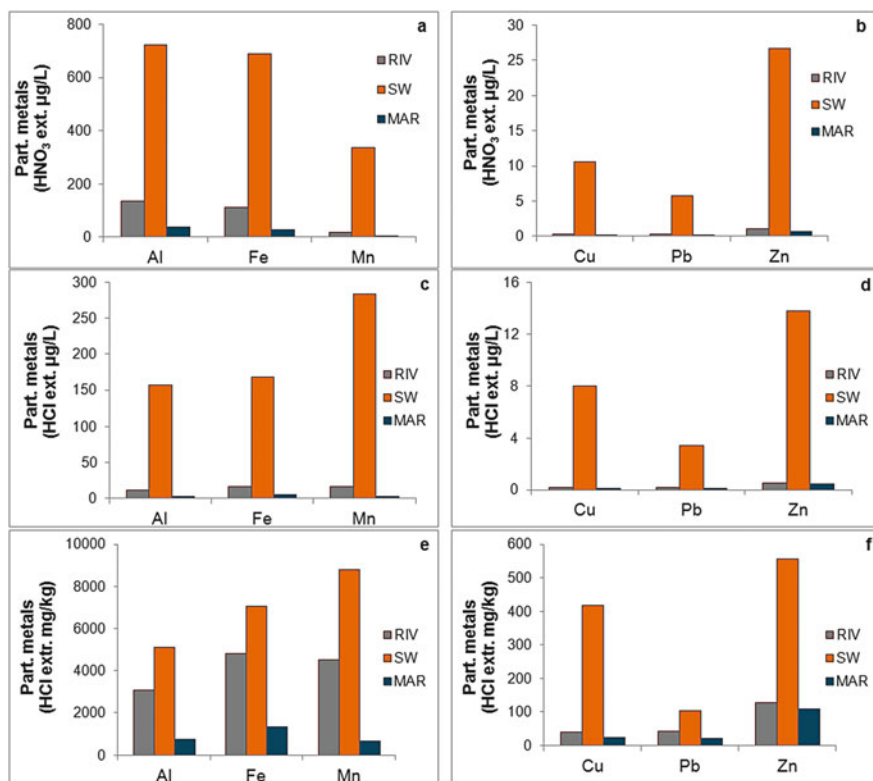
Fig. 5 Distribution of particulate metals in the riverine (RIV), the salt wedge (SW) and the marine (MAR) water masses of the Louros Estuary. (**a, b**): extracted by conc. HNO_3 (w/v); (**c, d**) extracted by 0.5 N HCl (w/v); (**e, f**) extracted by 0.5 N HCl (w/w)

conc. HNO_3, shows that for both fractions the particles of the marine water mass (**c**) have lower metal content than the riverine ones of water mass (**a**). Furthermore, Mn, Cu, Pb and Zn contents are the highest in the water mass (**b**) (Table 2). The parallel trend for the HNO_3 and HCl leachates of Mn, Cu and Zn is attributed to the fact that a considerable portion of the particulate metal is readily dissolved in dil. HCl; Mn extracted by the dil. HCl represents $83 \pm 9\%$ (mean $\pm$ sd) of Mn extracted by conc. HNO_3 ("pseudototal"); the HCl extractable fraction of particulate Cu and Zn represent $65 \pm 26\%$ and $64 \pm 18\%$, respectively, of the HNO_3 extracted metals.

Particulate Al and Fe contents extracted by conc. HNO_3 are reduced towards the marine sector of the system (Table 2). This seaward decreasing trend could be explained by mixing of fluvial, mineral particles with marine ones, which during summer, and low flow regimes are usually characterised by an increased contribution of the planktonic component in the overall suspended load [7, 9]. However, when considering the 0.5 N HCl leachable Al, Fe and Mn contents (Fig. 5e) it becomes evident that the highest values are found in the particles of water mass (**b**). This finding indicates the addition of Al, Fe and Mn forms that are easily extracted

by dil. HCl in the salt wedge. At the "salt-stress" surface, which separates water mass (**a**) from (**b**), the low pH Louros water meets the saline water of relatively higher pH. Formation of authigenic particles, especially Fe and Mn oxyhydroxides, is known to take place in similar interfaces [4, 15, 53], resulting in the enrichment of these metals in the particles of the salt wedge. In water mass (**b**), the extractability of Al by the 0.5 N HCl increases to $20 \pm 7\%$ compared to $8 \pm 5\%$ and $6 \pm 3\%$ in water masses (**a**) and (**c**), respectively. Thus, the observed Al-enrichment of the HCl-soluble fraction in water mass (**b**) could be related to the precipitation of Al-oxyhydroxides, or most probably to coagulation of fine, poorly crystalline aluminosilicates under the influence of increased ionic strength.

In order to gain insights into the solid-dissolved phase interactions, the partition coefficient K_D is employed, which is defined as follows: K_D = Particulate metal concentration (w/w)/Dissolved metal concentration (w/v) [16]. Summary statistics of K_D in the three water masses of the system is shown in Table 2.

Average K_D for each element decreases in the order Fe > Mn > Pb > Zn > Cu, indicating the affinity of Fe and Mn for the solid phases, whereas the lower K_D for Cu and Zn indicates their affinity for the dissolved phase. Similar K_D values are reported in other European Estuaries (Table 2), as reviewed by Balls [52]. The K_D values for Fe, Cu and Pb gradually decrease from the riverine water mass to the salt wedge and then to the marine water mass, whereas the K_D for Mn and Zn substantially decreases at the salt wedge in relation to the river water and further increases at the marine water mass. Characteristic plots K_D for Fe and Mn with salinity are shown in Fig. 6a, b.

The highest K_D values for Fe are found at the riverine water mass. Although coagulation of colloidal Fe could be significant at salinities of <5‰ [54], as dissolved Fe does not follow any clear trend with increasing salinity, addition of Fe from local sources at the low reaches of the Louros Estuary seems to be responsible for the elevated K_D values at this part of the system. Further downstream, the K_D for Fe decreases compared to the riverine water mass. This is despite the precipitation of Fe oxyhydroxides at the salt wedge, which was discussed previously. It should be noted that the particulate metal contents extracted by the boiling conc. HNO_3 are used for the calculation of K_D. Thus, the authigenic component of Fe in the pseudototal content is masked by the increased contribution of other mineral Fe-bearing phases, such as clays and crystalline oxyhydroxides. Apparently, addition of Fe in solution takes place at the salt wedge that is responsible for the decreased K_D values at this part of the system.

Sediment–water interactions and benthic fluxes could be an important source of dissolved metals, particularly in (periodically) anoxic or suboxic systems [5, 18, 55, 56]. The onset of anaerobic conditions due to initial oxygen consumption during organic matter decomposition results in the formation of metal authigenic sulfides and/or carbonate phases. These phases are stable under anaerobic conditions. There are two mechanisms responsible for the benthic fluxes of metals [55]: Firstly, metals may be released by molecular diffusion from pore waters. The diffusion is enhanced by higher temperatures and/or formation of dissolved metal species (e.g. Fe(II), Mn(II)) by reductive dissolution of Fe/Mn oxyhydroxides. In this way,
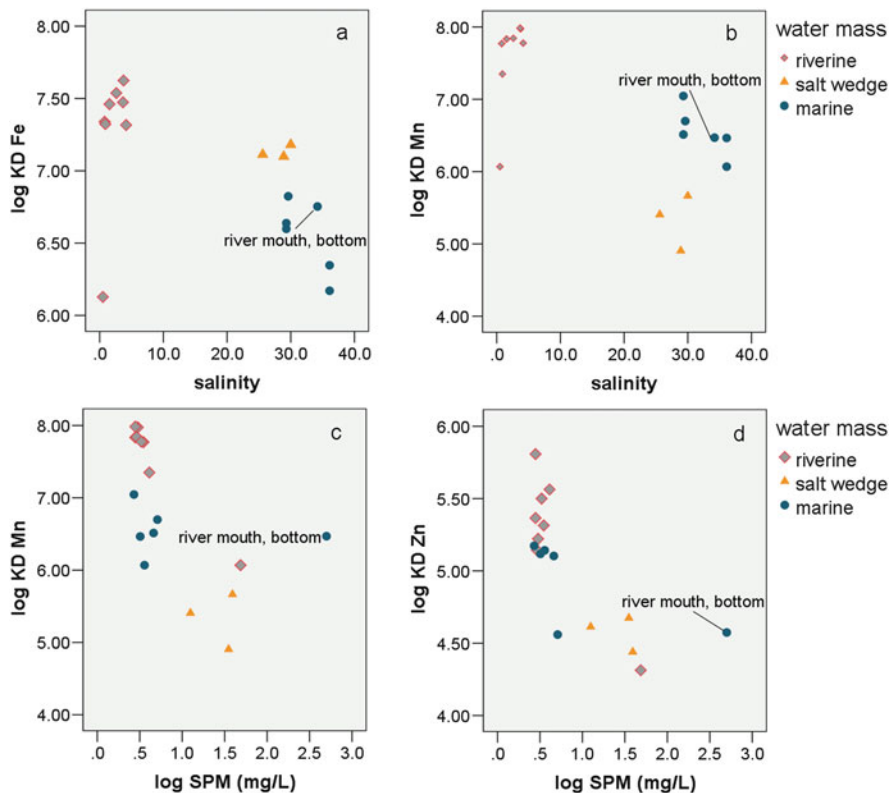
Fig. 6 Plots of partition coefficients (K_D) for Fe (**a**) and Mn (**b**) against salinity and K_D for Mn (**c**) and Zn (**d**) against suspended particulate matter (SPM)

trace metals previously bound to Fe/Mn oxyhydroxides could also be transported to the dissolved phase. Secondly, metal fluxes can be enhanced by physical, biological disturbances of sediments, i.e. re-suspension during flooding events and/or bioturbation, or salt wedge migration. In this case, apart from direct injection of pore waters into the water column, desorption from the suspended particles, oxidative dissolution of reduced authigenic solid phases (e.g. sulfides) could result in increased dissolved metal concentrations.

The observed further decrease of K_D for Fe (as well as Cu and Pb) at the marine water mass is attributed to the dilution of enriched riverine particles with marine, metal-poor particles of biogenic origin. This is supported by the decreased metal contents of suspended particles (in the w/w expression). Additionally, re-suspension of sediments, followed by emanation of dissolved metal species from pore waters into the water column and most probably desorption of metals from the re-suspended sediments, might also be responsible for high dissolved metal concentrations and the decrease of K_D for these metals. Re-suspension of sediments evidenced by the high SPM concentrations (500 mg/L) and subsequent

effects on the partitioning of Fe and trace metals between the solid phase and solution is best distinguished at the bottom water outside the river mouth (see Figs. 4 and 6a).

Similar processes could account for the variability of K_D for Cu and Pb along the three distinct water masses of the system. The increased dissolved metal concentrations observed in the salt wedge (Fig. 4) result in the decrease of K_D for these metals. Apart from the sediment–water interactions, previously described for Fe, desorption from suspended particles is an important mechanism releasing trace metals into the bottom, salt water mass. In this part of the system, the percentages of easily (0.5 N HCl) extractable particulate metals in relation to the pseudototal (HNO_3 extractable) content decrease compared to the riverine water, from 73% to 62% for Cu and from 66% to 62% for Pb. This finding suggests that weakly bound metals to suspended particles are released in solution. Desorption of metals is enhanced by the entrapment of suspended particles at the salt wedge, evidenced by the increased concentrations of SPM, and the long residence time of suspended particles during periods of low flow regime.

The partition coefficient K_D for Mn and Zn show an inverse relationship with SPM (Spearman correlation coefficients $r = -0.737$; $p = 0.001$ and $r = -0.771$; $p < 0.0005$, respectively), which is graphically illustrated in Fig. 6b. This relationship, known as particle concentration effect, has been observed in many estuaries (e.g. [2, 7, 57]). Several causes have been proposed for the decline of K_D with the increase of SPM concentrations, including the abundance of coarse particulate matter in occasions of high SPM load, which have lower surface area, hence fewer complexation/sorption sites per mass, the pronounced removal of trace metals in the estuarine turbidity maximum [58], but most often the existence of colloidal particles of <0.45 μm size that are counted with the dissolved fraction [59]. With increasing concentrations of SPM, the concentration of fine-sized colloids increases. These colloidal particles are able to bind metals and retain them in solution, hence the "dissolved" metal concentrations increase and K_D values decrease [7].

Part of the fine-sized colloidal particles could be removed from solution after coagulation under the influence of increased ionic strength. By conducting laboratory mixing experiments Sholkovitz [60] showed that the removal of Mn levels at salinities between 15 and 25‰, and additional removal occurs at salinities between 27 and 30‰. Thus, removal of Mn (and Zn) from the solution at the high salinity, marine water mass, combined with re-suspension of sediments, likely explain the observed increase of K_D for these metals from the salt wedge to the marine waters.

The surface sediments of the Louros Estuary are fine grained, with the mud fraction representing more than 95% of the entire sediment throughout the system. The organic carbon content increases from 0.6% in the upper part of the river to approximately 2.3% at the intermixing zone. The carbonate content does not fluctuate significantly along the system and ranges from 28% to 33%.

Table 3 summarises the results of extractions by conc. HNO_3 and 0.5 N HCl of surface sediment samples of the Louros Estuary. Compared to the composition of upper continental crust (UCC; [61]), Cu and Zn contents of the Louros surface

Table 3 Ranges and average (in parenthesis) of Al, Fe and trace metal contents in the surface sediments at the riverine and marine sector of the Louros system (number of samples, $n = 12$)

	Al		Fe		Mn		Cu		Ni		Pb		Zn	
	HCl	HNO₃	HCl	HNO₃	HCl	HNO₃	HCl	HNO₃	HCl	HNO₃	HCl	HNO₃	HCl	HNO₃
RIV (a)	0.25–0.37 (0.29)	1.42–5.05 (3.05)	0.45–1.00 (0.72)	1.35–4.05 (2.29)	350–760 (511)	390–870 (618)	18.5–38.3 (29.0)	28.8–51.9 (38.6)	42.0–87.8 (61.8)	113–242 (178)	5.50–11.5 (7.88)	6.10–13.0 (9.42)	24.2–79.2 (40.3)	36.1–107 (79.9)
SW (b)	0.28–0.35 (0.33)	3.65–5.05 (4.30)	0.84–1.00 (0.95)	2.24–4.05 (3.10)	510–760 (573)	610–810 (733)	31.0–38.3 (33.8)	42.5–51.9 (47.1)	42–64.6 (63.2)	183–242 (214)	7.80–8.60 (9.30)	10.6–13.0 (11.9)	24.2–79.2 (43.6)	89.4–107 (95.5)
MAR (c)	0.24–0.31 (0.27)	1.84–3.19 (2.55)	0.53–0.75 (0.53)	1.45–3.25 (2.47)	350–380 (370)	420–640 (513)	20.0–25.8 (23.4)	26.0–38.9 (33.3)	40.4–69.2 (51.1)	116–200 (168)	4.10–10.1 (7.33)	7.20–11.8 (9.27)	26.6–40.8 (31.6)	75.3–90.6 (82.3)
UCC	8.15		3.5		774		28		47		17		67	

The riverine sector includes stations located landwards of the sill bar and those overlain by the salt wedge development at the specific time of sampling, whereas the marine sector includes stations located seawards of the sill bar. For comparison with the composition of SPM, sediment samples of the salt wedge at which saline bottom waters were sampled are also given separately (b). Sediment samples were extracted by 0.5 N HCl (HCl) and boiling conc. HNO₃ (HNO₃). Al and Fe contents are given in % (w/w), whereas trace metal contents in mg/kg. For comparison we report also the average metal contents of the upper continental crust (UCC) reported by Rudnick and Gao [61]

sediments are slightly higher than the UCC, whereas Pb levels are lower than the UCC values.

Sediments of the riverine sector contain higher amounts of both fractions of metals than those of the marine sector. The percentages of Al extracted by the diluted HCl in relation to the conc. HNO_3 are stable across the system and have an average value of 11%, indicating common sources of Al throughout the estuary. This observation, combined with the fact that Al contents (HNO_3 extractable) decrease from 1.42–5.05% to 1.84–3.19% seawards, signifies that part of the fine-sized aluminosilicates are entrapped at the upper estuary due to presence of the sill bar (Fig. 3). The same pattern is observed for Fe and Mn as well. The extractability of Fe and Mn decreases from 34% and 84% at the riverine sector to 22% and 74% at the marine sector, respectively. This suggests that Fe/Mn oxyhydroxides (easily extractable with both acids), part of which are authigenically formed at the fresh–saline water interface, are also entrapped landwards from the sill bar. As clays and Fe/Mn oxyhydroxides are efficient scavengers for trace metals [47], the physical entrapment of these phases could also explain the relative enrichment of trace metals at the riverine sediments.

Sediments obtained from the stations affected by the active salt wedge at the time of sampling contain higher amounts of Al and Fe, but much lower amounts of metals compared to the overlying suspended matter (see metal contents of the SW sector in Tables 2 and 3). Apparently, the enrichment of the suspended particles during low flow conditions is reflected only to a small degree at the surface sediments that represent a long-term and variable flow regimes repository.

After normalising the metal contents to Al, in order to compensate for grain-size effects, a different distribution pattern of trace metals emerges. Figure 7 shows that higher metal to Al ratios are observed at the outer, marine sector of the Louros system. Thus, it is proposed that particles enriched in trace metals during their entrapment in the salt wedge by the processes described previously are transported and eventually accumulated seawards, during high flow regimes and flooding events.

Figure 8 illustrates representative vertical distributions of the HNO_3 extractable fraction of Cu in short cores obtained from the intermixing zone and an offshore station. It is clear that, despite the variability of the metal content at the various sites sampled, there is a general increase of Cu content towards the younger, surface sediments. This trend, which is also followed by Zn, Cr and Pb [28], suggests a gradual increase of pollution from a combination of small point and non-point sources.

Previous detailed mineral magnetic studies at the Louros Estuary [46], showed that the upper part of the cored sediments is dominated by fine grained, soil-derived material, rich in secondary spinel oxides, whereas the lower part of the cores has a much harder demagnetisation behaviour, which is attributed to the presence of hematite-coated sand grains clearly of detrital origin. The latter magnetic component has a different provenance, or derives from an earlier denudational regime. According to the study of Scoullos and Oldfield [46], Cu, among other metals, correlates with volume-specific magnetic susceptibility k and frequency dependent
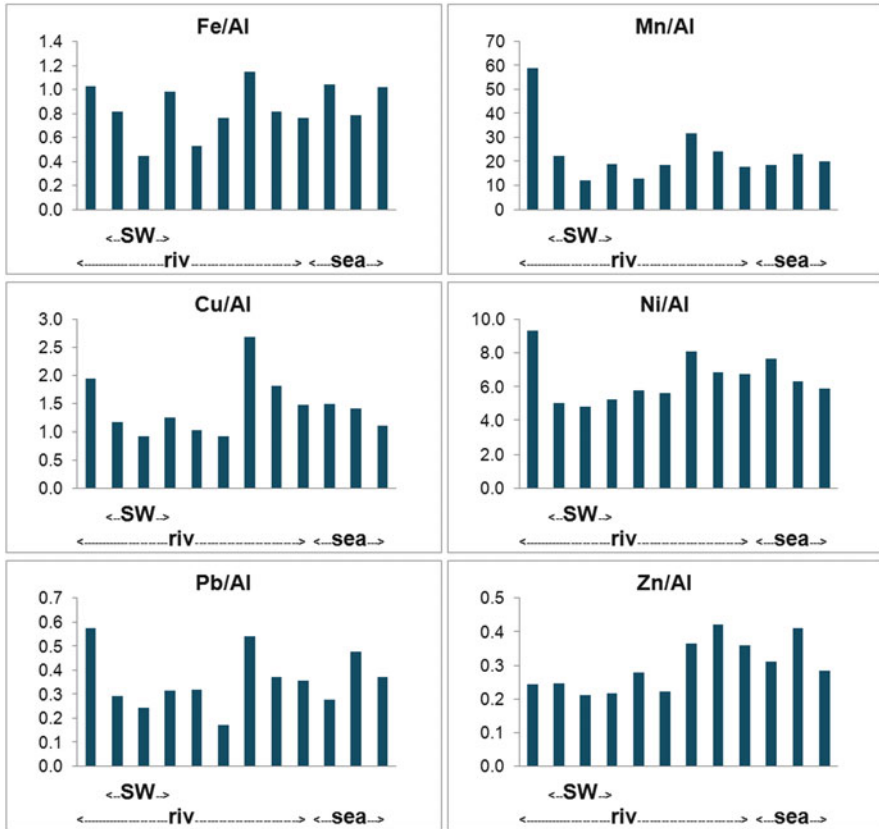
Fig. 7 Distribution of metal contents, extracted by boiling conc. HNO_3, normalised to Al (metal/Al) in the surface sediments of the Louros Estuary

magnetic susceptibility kfd%, only in one of the major components of the system, namely the fine particles deriving from soil erosion, predominantly found at the upper part of the cores. It is well known that the fine fraction of particles is the most important one for the transport of metals [47]. It is, thus, concluded that the enrichment of the surface layers of the cores is attributed to the transport of metals through land washout and runoff, with some contribution of the re-precipitation of dissolved metals occurring at the upper layers of the cores.

Summarising the results of the Louros system, a mechanism of metal enrichment within the intermixing zone could be proposed: After the separation of the heavier particles by precipitation at the upper part of the river, the lighter ones, with small grain sizes and higher content of metals, organic matter and minerals, remain in suspension until they reach the lower part of the estuary. A large proportion of these particles are accumulated at the stable fresh–saline water interface and at the thin intermixing zone and is then trapped and recycled within the landward moving saline layer, along the river bed (the salt wedge). Desorption of metals from mineral
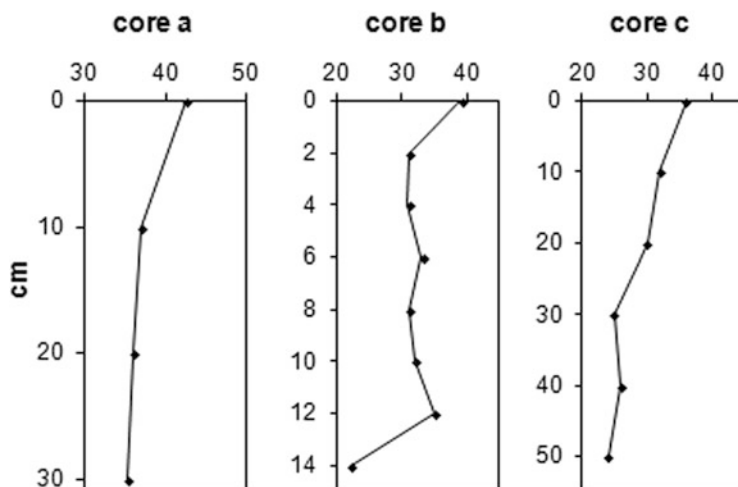
Fig. 8 Vertical distribution of Cu contents (in mg/kg) extracted by boiling conc. HNO$_3$ in cored sediments obtained from the estuarine (cores **a**, **b**) and the marine sector (core **c**) of the Louros River

surfaces of suspended particles (SPM) and/or re-suspended sediments, as well as benthic fluxes driven by diagenetic, redox processes in sediments, which provide the observed increases of dissolved metal concentrations in the salt wedge, is paralleled by an almost simultaneous formation of authigenic particles and colloidal, most probably Fe/Mn oxyhydroxides and Al clays. The metals trapped into the salt wedge can be released in the Amvrakikos Gulf when the river flow increases and the Louros Estuary becomes flooded.

4.2 The Acheloos Estuary

Based on the physicochemical and hydrological conditions, water samples obtained from the river course of Acheloos are divided into four types:

(a) The overflowing, seaward moving, riverine water mass, which includes samples of salinity <3 and water depth 0–0.5 m.
(b) The estuarine water mass, which includes samples of salinity 6.4–33.6 and water depths 0–5 m.
(c) The salt wedge, occupying the subsurface layer near the river bed, which includes samples of salinity 11.4–37.8 and water depths ranging from 1 to 5 m.
(d) The marine water outside the river mouth, which includes samples of salinity 36.1–38.1 and water depth 0–40 m.

Table 4 summarises the ranges and average values of Al, Fe and trace metals in the dissolved and particulate (extracted by conc. HNO$_3$ in w/w) phase in the

Table 4 Ranges and average (in parenthesis) concentrations of Al, Fe and trace metals in the dissolved (Diss.) and particulate (Part.) phase, as well as partition coefficient (K_D) in the four distinct water masses of the Acheloos system ($n = 128$)

	Al	Fe	Mn		Cu		Pb		Zn	
	Part	Part.	Diss.	Part.	Diss.	Part.	Diss.	Part.	Diss.	Part.
RIV (a)	0.15–6.46 (3.66)	0.10–4.32 (2.28)	0.03–2.75 (0.49)	797–6,283 (2,202)	0.01–5.40 (0.84)	4.2–110 (45.4)	0.07–2.85 (0.47)	8.1–130 (39.5)	0.28–21.7 (5.88)	126–2,609 (576)
EST (b)	0.54–5.25 (2.88)	0.49–3.91 (2.12)	0.04–2.50 (0.26)	333–4,049 (1,123)	0.20–2.99 (0.73)	9.9–123 (55.5)	0.06–2.23 (0.35)	9.8–721 (76.2)	0.40–35.1 (6.27)	67–4,019 (815)
SW (c)	0.63–3.10 (1.93)	0.24–3.35 (1.93)	0.04–2.69 (0.58)	259–4,152 (1,997)	0.03–0.90 (0.23)	3.9–104 (35.8)	0.11–4.13 (0.39)	7.7–814 (123)	3.90–21.8 (12.1)	180–2,771 (636)
MAR (d)	0.05–2.05 (0.54)	0.06–2.09 (0.46)	0.03–0.80 (0.25)	21–2,000 (406)	0.11–2.83 (0.62)	3.8–471 (106)	0.11–4.13 (0.39)	9.6–580 (91.1)	0.55–46.5 (3.53)	50–6,170 (1,013)
K_D										
RIV (a)			5.84–7.76 (7.03)		3.15–6.29 (4.98)		3.64–5.80 (4.99)		4.31–6.04 (5.16)	
EST (b)			6.03–7.53 (6.84)		3.84–5.52 (4.90)		4.61–6.04 (5.26)		4.08–6.73 (5.09)	
SW (c)			5.02–7.84 (6.91)		3.96–6.42 (5.20)		4.29–6.14 (5.01)		4.12–5.45 (4.59)	
MAR (d)			4.93–7.24 (6.05)		3.84–6.53 (5.16)		3.83–6.08 (5.20)		4.10–6.47 (5.30)	

Dissolved metal concentrations are expressed in µg/L. Particulate metal contents are expressed in % for Al and Fe and in mg/kg for trace metals. K_D is expressed in logarithmic values. The marine sector includes samples obtained from the surface and from 10, 20 and 40 m depths

aforementioned water masses of the Acheloos system. Dissolved Mn and Cu concentrations are lower than the average values of World's Rivers reported by Viers et al. [51] (Table 2), whereas Pb and Zn are higher. Average particulate metal contents are lower than the world's average values, except for Zn. The Acheloos River receives land runoff from a large catchment area, influenced by agricultural activities and atmospheric depositions, and probably urban effluents from small cities. Nevertheless, compared to other large perennial Greek rivers, the Acheloos system could be characterised as relatively unpolluted [32].

Considering the variations of dissolved metal concentrations in the four water masses of the system, on average, the highest concentrations of metals, except Cu, are determined in the salt wedge (Table 4). The addition of Mn and Pb in solution at the salt stress interface is related to interactions between the dissolved phase and suspended particles and/or re-suspended sediments. Based on the average values, dissolved Cu decreases from the riverine to the estuarine water mass and the salt wedge and further increases at the marine waters. Occasionally, deviations from these general distribution patterns are observed, when distinct sampling cruises are considered. Figure 9a shows the plots of dissolved metal concentrations with salinity during one month in the summer. In this case, dissolved Cu, Pb and Zn concentrations increase with increasing salinity in the estuarine zone, either gradually (Cu, Pb) or locally (Zn). Dissolved Mn concentrations do not vary widely between the riverine and the estuarine water mass. Nevertheless, the most interesting feature is probably the increased dissolved Mn, Cu and Pb concentrations in the marine waters, indicating that release processes occur not only in the intermixing zone, but also in the outer, marine stations of the system.

Figure 10 shows the distribution of average SPM and particulate metal concentrations in the four water masses of the system, as well as the plots of SPM, and particulate metals (in the w/v expression) with salinity during one month in the summer. On average, SPM concentrations decrease seawards due to dilution and deposition of coarse-grained fluvial particles before, or around the sill bar at the river's mouth [32]. High concentrations are determined at the bottom water of the salt wedge, due to re-suspension of sediments and trapping of settling particles, which is clearly depicted when a single sampling cruise is considered.

Average particulate Al, Fe and Mn concentrations (in the w/v expression) follow the distribution of SPM (Fig. 10a). They vary widely in the river water, in response to the hydrological regime, decrease in the estuarine mass but become enriched in the salt wedge, and further decrease in the marine waters. Particulate Cu and Pb are enriched in the estuarine waters and the salt wedge. These general distribution patterns are observed when a single sampling is considered, too (Fig. 10b). Particulate Zn does not vary greatly between the four masses of the system. During the summer month, the highest Zn concentration is determined at a marine station, probably due to the uptake of this element by phytoplankton.

Particulate Al and Fe contents (in the w/w expression) decrease gradually seawards, due to dilution of fluvial particles with biogenic, Al/Fe- poor, marine particles (Table 5). Particulate Mn exhibits its highest values in the riverine water mass and the salt wedge. The enrichment of particulate Mn probably indicates the
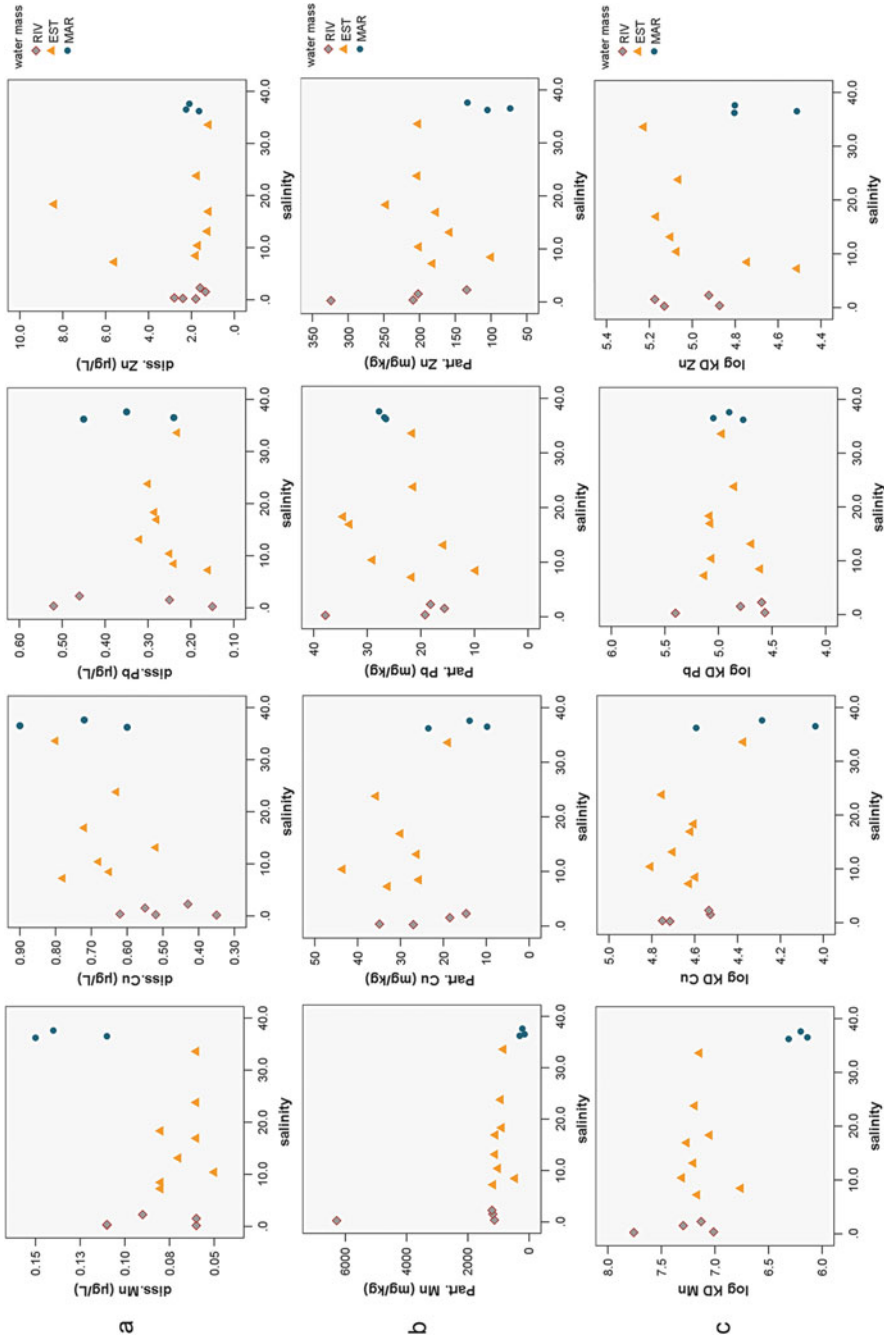
Fig. 9 Plots of (**a**) dissolved metal concentrations; (**b**) particulate metal contents (w/w); (**c**) partition coefficients K_D for Mn, Cu, Pb and Zn with salinity in the Acheloos system during a summer month
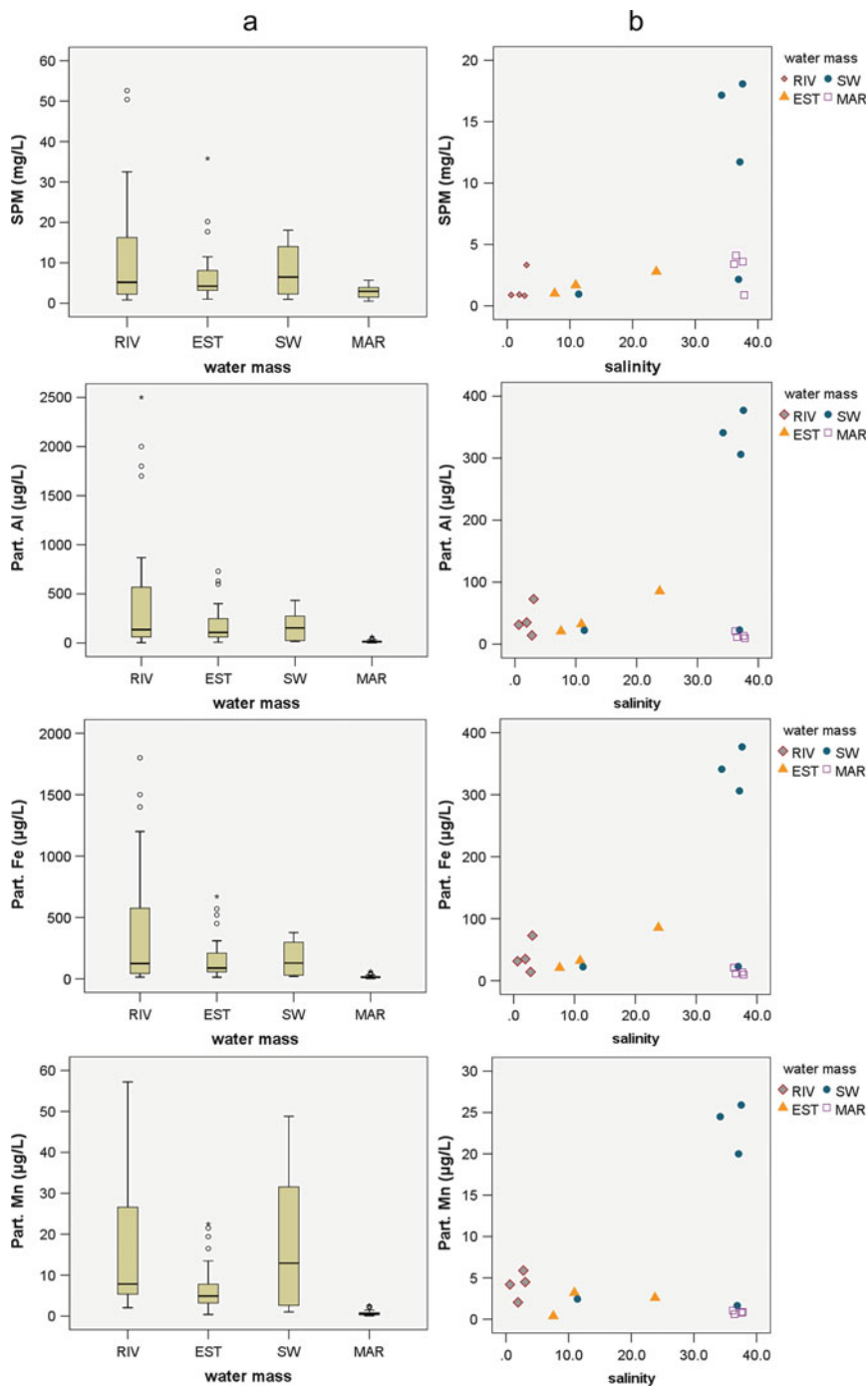
Fig. 10 Distribution of SPM and particulate metal concentrations (w/v) in the four water masses of the Acheloos Estuary: (**a**) Boxplots in the *left panel* summarise statistic data of all samplings; (**b**) scatter plots in the *right panel* show the variations of the studied parameters with salinity during a summer sampling cruise
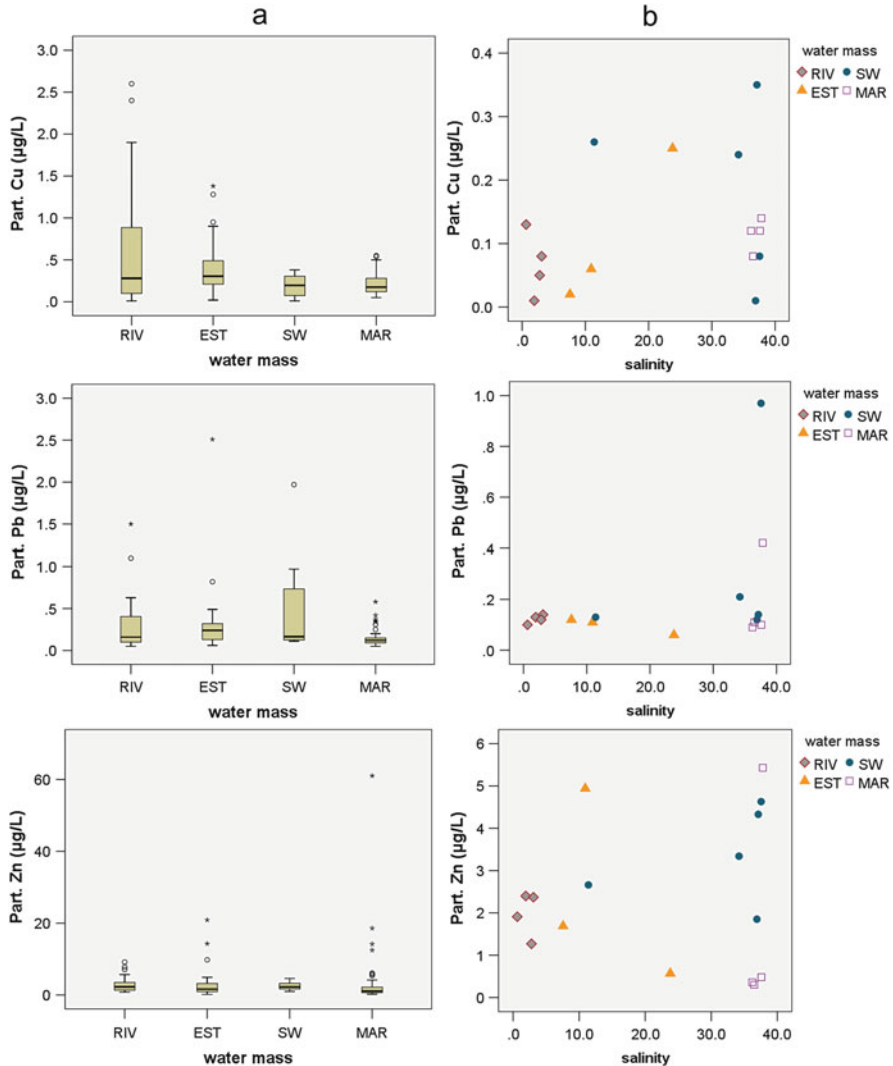
Fig. 10 (continued)

formation of authigenic Mn oxyhydroxides [32]. Particulate Cu, Pb and Zn are enriched, either in the estuarine water mass or the salt wedge. Scavenging by Mn oxyhydroxides or re-suspension of sediments are the likely sources of Cu, Pb and Zn enriched particles.

Figure 9c shows the variation of partition coefficient (K_D) for Mn, Cu, Pb and Zn as a function of salinity during a summer cruise. By combining the distribution patterns of K_D with those of dissolved metal concentrations (Fig. 9a) and particulate metal contents (Fig. 9b), some interesting observations on solid–solution interactions might be deduced.

Table 5 Ranges and average (in parenthesis) of Al, Fe and trace metal contents of the surface sediments at the five zones of the Acheloos Estuary (number of samples, n = 14)

Zone	Al HCl	T	Fe HCl	T	Mn HCl	T	Cu HCl	T	Pb HCl	T	Zn HCl	T
A	0.12–0.30 (0.23)	2.08–2.98 (2.41)	0.13–0.66 (0.36)	1.28–1.80 (1.57)	410–650 (550)	500–660 (597)	21.8–24.3 (23.1)	25.5–31.3 (28.8)	6.2–9.9 (7.6)	7.6–12.4 (9.9)	16.4–24.0 (19.8)	44.2–57.6 (49.7)
B	0.02–0.06 (0.05)	0.56–0.86 (0.74)	0.14–0.24 (0.20)	0.52–0.89 (0.74)	400–500 (463)	480–560 (520)	4.20–11.0 (7.53)	10.1–13.0 (11.6)	2.5–3.6 (3.0)	5.8–7.0 (6.2)	8.6–15.9 (11.6)	28.8–43.4 (37.0)
C	(0.28)	(2.80)	(0.41)	(1.91)	(380)	(470)	(26.2)	(38.4)	(9.7)	(11.3)	(25.6)	(81.7)
D	0.04–0.06 (0.05)	0.45–0.71 (0.53)	0.09–0.18 (0.14)	0.24–0.49 (0.38)	520–680 (625)	560–730 (663)	3.70–11.6 (5.90)	7.0–12.9 (9.4)	2.4–3.3 (2.8)	3.7–6.2 (5.0)	7.2–22.2 (15.3)	24.8–45.3 (32.5)
E	(0.28)	(3.96)	(0.45)	(2.50)	(470)	(510)	(20.5)	(32.3)	(14.4)	(15.1)	(34.9)	(72.8)

Zone A represents the upper estuary where the upper boundary of the salt wedge is observed during the low flow seasons; zone B extends over the area where the salt wedge is observed most of the time; zone C consists of a single station located at the river mouth and the sill bar; zone D is the lower estuary, off the river's mouth; zone E consist of one offshore station of the lower estuary. Sediment samples were extracted by 0.5 N HCl and conc. HNO_3:$HClO_4$ (T). Aluminium and Fe contents are given in % (w/w), whereas trace metal contents in mg/kg

Similar to the Louros Estuary, dissolved Mn increases at the low salinity (<10) regime. At the riverine and the estuarine water masses the partition coefficient K_D for Mn is inversely correlated to SPM (Spearman correlation coefficient $r = -0.556$; $p = 0.046$), indicating that the increased dissolved Mn concentrations correspond to increased colloids rather than truly dissolved forms (particle concentration effects). Colloidal Mn oxyhydroxides could be transferred seawards, or deposited at the estuarine zone after coagulation, depending on the river's flow regime. According to Dassenakis, Scoullos and Gaitis [32] these forms, together with Mn and Fe oxyhydroxides coating small particles and clays, are the main carriers for trace metals in the Acheloos system. The K_D for Mn decreases sharply at the outer marine stations. This decline is accounted for by the combined effect of the elevated dissolved Mn concentrations at the marine stations and the reduction of particulate Mn contents. Therefore, it is suggested that desorption processes and dilution of fluvial particles with the marine ones are taking place almost simultaneously. In the case of Cu, the increase of K_D at the mid-salinity regime is attributed to the increased particulate Cu contents, which likely ascribe to re-suspension of sediments. This is despite the increase of dissolved Cu concentration in the same region. Probably, the addition of Cu enriched particles from the sediments masks desorption processes. Similar processes could explain the variations of K_D for Pb, and Zn at the low- and mid-salinity regimes. Nevertheless, the most remarkable observation for all the elements presented in Fig. 9 is the elevated dissolved concentrations at the marine stations, which in combination with the decrease of K_D values, signify the importance of desorption processes at this part of the system.

At the marine stations, water samples were obtained from the surface, from 20 m and 40 m depth of the water column. The variations of SPM, particulate Al, dissolved and particulate Pb, as well as its partition coefficient with depth during a spring and a summer month (the same as in Fig. 9) are shown in Fig. 11a, b, respectively. The concentration of suspended particles varies with depth and increases either at both subsurface layers (spring; Fig. 11a) or at 40 m (summer; Fig. 11b). Particulate Al does not follow the distribution of SPM, suggesting the increased contribution of biogenic particles to the overall suspended load. Re-suspension of sediments could be an additional source of particles at the near-bottom waters, particularly during spring, when increased SPM concentrations are accompanied by increased Al contents at 40 m depth. Dissolved Pb concentrations are higher in the subsurface waters, than in the surface. At 40 m depth, oxic conditions prevailed during all samplings, with dissolved oxygen saturation ranging from 80% to 110% [32]. Thus, the increasing concentrations could not ascribe to benthic fluxes due to redox reactions. The K_D for Pb shifts to lower values with increasing depth of the water column, whereas particulate Pb follows the reverse trend. Release processes to the solution, which are evidenced by the decrease of K_D from the surface to the subsurface waters, suggest that desorption processes are taking place at the marine water column, due to competing and complexing processes with seawater ions. Increasing concentrations in solution with increasing depth of the water column are observed for Mn, Cu and Zn and desorption processes are recognised for these elements, too [32]. The abundance of organic ligands in
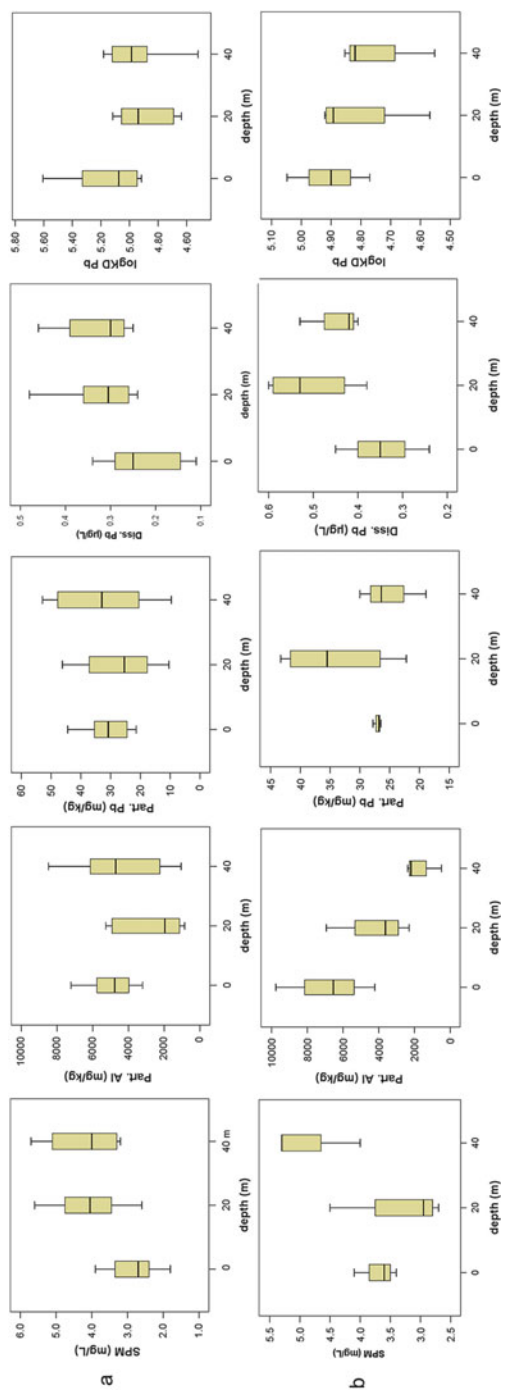
Fig. 11 Variations of SPM, particulate Al and Pb (w/w) dissolved Pb and K_D for Pb in the water column of outer marine stations of the Acheloos River during (**a**) a spring and (**b**) a summer month

colloidal and dissolved forms could also enhance desorption from suspended solids [3]. Desorption is a slow process and is greatly affected by the size of the estuary [13]. Therefore, any further changes of the hydrological regime of the Acheloos River may have a great impact on the behaviour and fate of trace metals, not only in the fresh–saline water interface, but in the coastal marine environment as well.

Surface and core sediments were collected from the upper and lower part of the Acheloos Estuary (Fig. 2). A detailed description of textural and mineralogical composition, as well as information on the sampling network, is given in Dassenakis et al. [25]. Table 5 summarises the results of extractions by conc. HNO_3 and 0.5 N HCl of the surface sediment samples of the Acheloos Estuary in the aforementioned zones. Compared to the composition of the continental crust (UCC; [61]; Table 3) much lower Al, Fe levels are detected in the Acheloos system, because of the incomplete dissolution of the crystal lattice of aluminosilicates by HNO_3. In general, all other metals are lower than the UCC values, reflecting low levels of pollution, due to the absence of major urban and industrial waste water discharges from point sources.

For a better consideration of the spatial variation, the estuary is subdivided into the following zones: zone A represents the upper estuary where the upper boundary of the salt wedge is observed during the low flow seasons; zone B extends over the area where the salt wedge is observed most of the time; zone C consists of a single station located at the river mouth and the sill bar; zone D is the lower estuary, off the river's mouth; zone E consists of the offshore station of the lower estuary at the boundaries with the marine sector, where salinity exceeds 25 and the water depth is >20 m.

Average contents of carbonates and organic carbon (OC) in the five zones of the system are 27% and 2.3% (zone A); 38% and 1.2% (zone B); 25% and 2.5% (zone C); 51% and 0.5% (zone D); 24% and 2.1% (zone E), respectively. Apparent differences on the composition of sediments exist between the zones. Sediments of zones B and D contain higher amounts of carbonates, and lower amounts of organic carbon and Al, whereas sediments of zones A, C and E contain lower amounts of carbonates and higher amounts of organic carbon and Al. Aluminium, Fe, Cu, Ni, Pb and Zn follow a very similar spatial distribution pattern (range of Spearman correlation coefficients between Al and other metals r: 0.714–0.928). On the contrary, Mn follows the distribution of carbonates ($r = 0.633$; $p = 0.015$), therefore indicating that calcite minerals might act as nucleation centres for manganese oxides, since there is a microzone of higher pH on the surfaces of carbonates [25]. The identical patterns of distributions of OC, Al, Fe and trace metals signify that clay minerals, originating from soil erosion, serve as a host phase for OC, and Al, Fe rich phase [20]. These fine clays are effective carriers for trace metals [47]. Evidently, compositional differences play a significant role in the distribution patterns of "total" trace metals and after normalising to Al, the large variations between the zones become "smoother" to some extent. However, when considering the fraction of metals extracted by dil. HCl (Table 5), it is clearly illustrated that zones A, C and E are accumulation sites of labile metals.

The increased labile metal contents in zone E compared to zone D indicate that a significant part of metals is flushed out of the estuary and settles in the offshore

stations. Increased labile metal contents at zone A, where the end of the salt wedge is occasionally observed, could be ascribed to coagulation of particles in the "salt-stress" interface and subsequent sedimentation. Hydrodynamics and the geomorphology of the system also play a significant role. Zone C, which is a zone of trace metal accumulation, is located landward from the sill bar that could act as a natural barrier of particulates enriched by geochemical processes, at least under regular flow conditions. These particles could be recycled back to zones A and B at periods of low river discharge when seawater intrudes the upper part of the estuary, or flushed away under high river discharge conditions.

The impacts of changing hydrological regime on the distribution of metals, as well as of natural and/or anthropogenic activities in the Acheloos catchment area, could be depicted from the study of cored sediments.

Magnetic parameters in the bulk cored sediments of the Acheloos Estuary were studied by Scoullos and Oldfield [46] and allowed for the recognition of two major magnetic components: the first one of high magnetic concentrations and relatively softer demagnetisation behaviour corresponds to clay-like sediments, whereas the second population of particles, which corresponds to coarser, sandy sediments, appears to be richer in canted anti-ferrimagnetic grains (e.g. hematite) and probably has a deeper subsoil or bed-rock origin. Comparison of the vertical distributions of volume-specific magnetic susceptibility with 0.5 N HCl leachable fractions of Cu and Zn showed close similarities in their profiles in the clay-size sediments of (a) the lower reaches of the estuary upstream from the river mouth, and (b) in the upper layers (>12 cm depth) of the cores obtained from the mouth bar of the river. In the latter area, sediments of deeper layers are coarser, poorly correlated to the leachable fractions of metals and most probably reflect reworked littoral material from a different provenance, or an early denudational regime [46].

Figure 12 illustrates the vertical distributions of labile fractions of metals from a short core obtained from zone B, normalised to Al in order to compensate for grain-size effects. Sediments of the upper strata have higher metal contents or higher metal to Al ratio values. The same pattern is also observed in other cores obtained from the Acheloos Estuary [25]. Apart from direct, recent anthropogenic activities in the entire catchment area, another cause of the observed increase in the surface sediments seems to be the reduction of particulate load of the estuary. Before the construction of dams the inert, non-polluted matter, which originated from rock weathering and natural soil erosion, was mixed with authigenic precipitates, which originated from the reactions in the dissolved and particulate phase under changing physicochemical conditions. This authigenic suspended matter contains significantly higher concentrations of pollutants. After the construction of dams, there was a diminished frequency of floods capable of flushing out the system by transporting newly deposited authigenic sediments from the estuary to the sea. By changing the nature and the relative contribution of particles in the mixture of suspended sediments coupled with the minimisation of the fraction which comes from the mountains, the final composition of the naturally generated suspended matter becomes increasingly loaded with pollutants, such as trace metals.

The fractionation of metals in the sediments of zones A to E, following the sequential extraction procedure presented in Table 1, are shown in Fig. 13. More
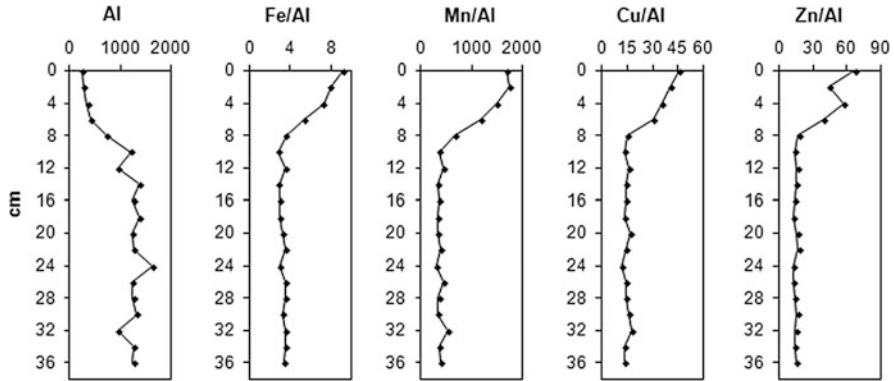
Fig. 12 Vertical distribution of 0.5 N HCl extractable Al and normalised metal ratios to Al, in cored sediments obtained from zone B
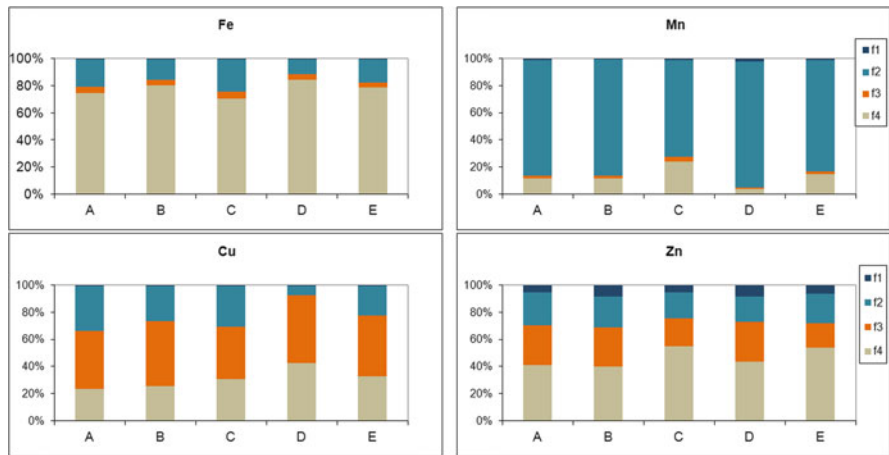
Fig. 13 Percentages of the geochemical fractions of metals in the surface sediments of zones A–E of the Acheloos system. The fractions of metals are F1: easily extractable; F2: non-lattice held, inorganic; F3: organic; F4: residual and are determined by following the sequential extraction procedure of Table 1

than 70% of "total" Fe content is lattice held. Manganese is mainly found in the non-lattice held inorganic fraction, which accounts for 71–93% of Mn total content, suggesting its presence as oxyhydroxides and bound to carbonates. The proportions of Cu and Zn are also elevated in the non-lattice held inorganic fraction consisting on average 23.6% and 21.4% of the "total" metal content. This indicates an increased mobility of these metals in the Acheloos Estuary. However, the dominant component of the "total" metal content is the non-lattice held organic fractions of Cu and Zn contributing on average 45.2% and 25.4% to the "total" contents.

A note should be made at this point about the limitations of sequential extraction procedures, including the non-selectivity of reagents, the potential redistribution of

metals among phases during extraction, or incomplete extractions [62]. The non-selectivity of reagents to attack only one solid phase is more profound when dealing with anoxic sediments, when metal sulfides are likely to occur. For example, Shannon and White [63] conducted laboratory experiments with known additions of synthetic iron oxyhydroxides (FeOOH), iron monosulfide (FeS) and pyrite (FeS$_2$) to natural freshwater lake sediment. The authors found that the extraction by the 0.04M NH$_2$OH·HCl in 25% acetic acid reagent at 96°C removed 25% of the Fe added as FeS, but it did not dissolve FeS$_2$. Furthermore, the same reagent was found to extract 50% of Zn which was present as ZnS [64]. In the case of the Acheloos sediments, we have no indication of anoxia (smell, black colour bands). Mineralogical analysis by X-ray diffraction (XRD) analysis showed that the main minerals present in the sediments were calcite, quartz, biotite, as well as illite and chrorite [25]. Therefore, metal sulfide minerals, if present, would exist in very small amounts, mainly in the subsurface sediments. In this case, these phases are expected to be extracted in the F2 fraction (the non-lattice held inorganic fraction) of the sequential extraction procedure.

Characteristic distributions of the exchangeable, inorganic and organic and the residual fractions of Fe and Cu in surface and subsurface sediments of cores obtained from the five zones of the system are presented in Fig. 14.

Comparison of the surface and subsurface sediments of the two cores obtained from zone A shows substantial variations with depth of labile Fe contents, dominated by Fe oxyhydroxides, and probably trace amounts of Fe sulfides, formed in situ by redox reactions. These differences suggest that the amount of Fe oxyhydroxides leached from soils of the upper catchment area and transported and subsequently accumulated in the upper estuary has changed over time, due to the combination of land-use changes and river discharge. In situ reductive dissolution of Fe oxyhydroxides is expected to contribute only to a small extent, hence, the variations of the non-lattice held inorganic fraction primarily reflect the long-term modification of oxyhydroxides inputs in this zone.

Moving downstream to zone C, at the sill bar, surface sediments contain much higher amounts of Fe oxyhydroxides than the subsurface ones, reflecting the relative enrichment of sediments by the authigenically formed oxyhydroxides favoured by the prolonged residence time of waters due to the reduction of river discharge and the influence of the salt wedge. The relative depletion of Fe oxyhydroxides at the subsurface sediments of zone C and the relative enrichment at the subsurface sediments of zones D and E signify that in the past, under a different hydrological regime of higher river discharge, the labile fraction of Fe was flushed away, off the river's mouth and accumulated in the offshore stations of the lower estuary. The same processes explain the relative depletion of labile forms of Cu in the subsurface sediments in the cores of zones C and D. In the surface sediments of zone D, an increase of the organic fraction of both Fe and Cu is observed. Different transport pathways of colloidal and particulate metals during their passage through the active mixing zone [20] or an in situ control (biological uptake) of an autochthonous component of organic matter [4] could be the possible reasons. The overall much lower amounts of all fractions of metals in the surface
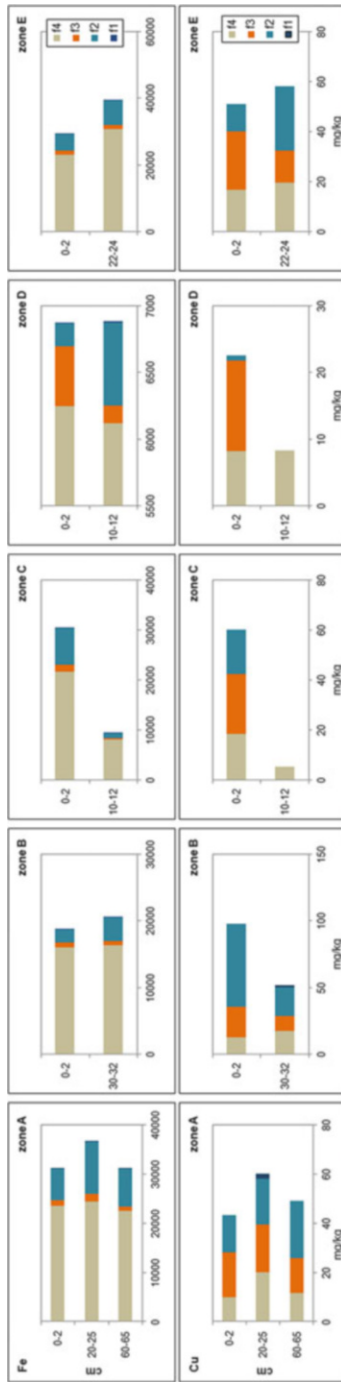
Fig. 14 Geochemical fractionation of Fe (*upper panel*) and Cu (*lower panel*), employing the sequential extraction procedure (1) described in Table 1, in cored sediment obtained from zones A (*left*) to zone E (*right*). Fraction F1: easily extractable; F2: non-lattice held, inorganic; F3: organic; F4: residual

and subsurface sediments of zone D in relation to other zones are attributed to the dilution due to the high carbonates contents, which in this zone are twice higher than in the other zones.

At the offshore station of zone E, the increased contents of labile Fe (and Cu to a lesser extent) of the subsurface sediments in relation the surface ones reflects more pronounced transport and deposition processes at this site in the past.

Putting together the variations of geochemical partitioning in the temporal and spatial scale, it can be proposed that there is propagation of the active mixing zone towards the inner part of estuary, where particles enriched in trace metals are deposited. This observation should be combined with the prediction ([34] and the references therein) that under reduced discharges of sediment, the sandy beaches and island barriers of the Acheloos delta will gradually erode and coastal lagoons will be intruded by seawater. These findings are important for the design of appropriate management measures of the area.

5   General Discussion and Conclusions

The Louros Estuary, which has a relatively narrow intermixing zone, low river flow and insignificant tides, has a saline water wedge intruding along the river and forming a small water mass, different from the riverine and the marine ones. The concentrations of dissolved and particulate metal species in this landward moving water body are considerably higher than in the other water masses. Physical entrapment of suspended solids landwards of the sill bar and the long residence time of suspended particles during periods of low flow regime, as well as re-suspension of sediments and subsequent benthic fluxes of metals or desorption from the suspended sediments, favour release processes of metals into solution. In the same region, new particles are formed authigenically, by precipitation of iron and manganese oxides and coagulation of clay minerals, at the interface of fresh and saline water. The accumulation of particulate metals in the salt wedge affects directly their distribution in the sediments, where the concentrations of some metals, including Al, exhibit their maxima. Although the zone of the salt wedge formation acts as trap of trace metals, the system should be considered as a periodic, (potential) source of metals for the adjacent sea, the Amvrakikos Gulf, particularly during flooding episodes.

Furthermore, the small size of the estuary, the shallowness and the low river flow indicate the vulnerability of its present, natural structures against changes. Pressures of local or global character could easily affect the borders of the fresh–saline water interface and transform the Louros Estuary into a secondary source of metals.

In the case of the much bigger and highly fragmented Acheloos River, the study reveals that the fresh–saline water interface is enriched in trace metals by re-suspension of sediments and desorption processes. Desorption of trace metals from the particles occurs in the intermixing zone, as well as in the offshore surface and subsurface marine waters, at 20 and 40 m depth, due to competing and

complexing effects of major seawater ions. Currently, a significant fraction of labile metals is accumulated in the upper part of the estuary, the sill bar and the offshore stations of the lower estuary. Although the river is not heavily polluted, temporal trends depicted from the study of sediment cores show that surface sediments are enriched in labile forms of metals, as a result of non-point anthropogenic sources, in combination with a considerable decrease of the water flow and floods (due to the construction and operation of dams), which in the past used to flush out recently deposited polluted sediments, "diluting" the authigenic and anthropogenic component by inert, non-polluted particles.

Modifications of the hydrological regime have resulted in the transfer of the intermixing zone towards the inner part of the estuary, where authigenic, rich in metals, particles are deposited. At the same time, decreased river discharges and sediment fluxes have narrowed the zone at which transport of labile metals takes place under regular flow conditions.

A further decline in water and sediment fluxes, in case of the proposed diversion of a portion of Acheloos waters towards Pinios river is realised, or due to climatic changes, may result in the development of a much stronger (in length and duration) salt wedge, intensifying the processes that are responsible for the relative enrichment of the trace metals in the estuarine zone. Then, episodic flooding of the estuary could release the finest, unconsolidated particles enriched in trace metals into the adjacent wetlands and the sea with a potential impact also on the biota through the food chain.

The results of the research carried out in the two unique, fresh–saline water interface systems are important not only in order to inform us about the geochemical processes in nature, but also in order to provide the necessary knowledge to properly manage these systems for the benefit of the environment and the sustainable development of the impacted areas. The existing provisions of the EU Water Framework Directive and the EU Marine Strategy Framework Directive suggest due attention to the processes in transitional zones described in this work. Furthermore, the Barcelona Convention Protocol for the Integrated Coastal Zone Management, as well as the Ecosystem Approach, point to the need for a thorough and systematic integration of research results into a combined management of coastal zones and water resources.

References

1. Bewers JM, Yeats PA (1989) Transport of river-derived trace metals through the coastal zone. Neth J Sea Res 23(4):359–368
2. Ollivier P, Radakovitch O, Hamelin B (2011) Major and trace element partition and fluxes in the Rhône River. Chem Geol 285:15–31
3. Roussiez V, Ludwig W, Radakovitch O, et al. (2011) Fate of metals in coastal sediments of a Mediterranean flood-dominated system: an approach based on total and labile fractions. Estuarine Coastal Shelf Sci 92(3):486–495

4. Guieu C, Martin JM (2002) The level and fate of metals in the Danube River Plume. Estuarine Coastal Shelf Sci 54(3):501–512
5. Jiann KT, Wen LS, Santschi PH (2005) Trace metal (Cd, Cu, Ni and Pb) partitioning, affinities and removal in the Danshuei River estuary, a macro-tidal, temporally anoxic estuary in Taiwan. Mar Chem 96:293–313
6. Shiller AM, Boyle EA (1991) Trace elements in the Mississippi River delta outflow region: behavior at high discharge. Geochim Cosmopolitica Acta 55:3241–3251
7. Zhou JL, Liu YP, Abrahams PW (2003) Trace metal bahaviour in the Conwy Estuary, North Wales. Chemosphere 51:429–440
8. Turner A, Millward GE, Le Roux SM (2004) Significance of oxides and particulate organic matter in controlling trace metal partitioning in a contaminated estuary. Mar Chem 88:179–192
9. Zwolsman JJG, van Eck GTM (1999) Geochemistry of major elements and trace metals in suspended matter of the Scheldt Estuary, Southwest Netherlands. Mar Chem 66(1–2):91–111
10. Horowitz AJ, Elrick KA (1987) The relation of stream sediment surface area, grain size and composition to trace element chemistry. Appl Geochem 2:437–451
11. Radakovitch O, Roussiez V, Ollivier P, et al. (2008) Input of particulate heavy metals from rivers and associated sedimentary deposits on the Gulf of Lion continental shelf. Estuarine Coastal Shelf Sci 77:285–295
12. Roussiez V, Probst A, Probst JL (2013) Significance of floods in metal dynamics and export in a small agricultural catchment. J Hydrol 499:71–81
13. Morris AW (1990) Kinetic and equilibrium approaches to estuarine chemistry. Sci Total Environ 97(98):253–266
14. Elbaz-Poulichet F, Garnier JM, Guan DM, et al. (1996) The concervatiive behaviour of trace metals (Cd, Cu, Ni and Pb) and As in the surface plume of stratified estuaries: Example of the Rhone River (France). Estuarine Coastal Self Sci 42:289–310
15. Fu J, Tang X, Zhang J, Balzer W (2013) Estuarine modification of dissolved and particulate trace metals in major rivers of East-Hainan, China. Cont Shelf Res 57:59–72
16. Turner A, Millward GE (2002) Suspended particles: their role in estuarine biogeochemical cycles. Estuarine Coastal Shelf Sci 55:857–883
17. Puig P, Palanques A, Sanchez-Cabeza JA, Masque P (1999) Heavy metals in particulate matter and sediments in the southern Barcelona sedimentation system (North-western Mediterranean). Mar Chem 63:311–329
18. Zwolsman JJG, van Eck GTM, Van Der Weijden CH (1997) Geochemistry of dissolved trace metasl (cadmium, copper, zinc) in the Scheldt Estuary, Southwestern Netherlands: Impacts of seasonal variability. Geochim Cosmochim Acta 61(8):1635–1652
19. Nolting RF, Helder W, De Baar HJW Gerringa LJA (1999) Contrasting behaviour of trace metals in the Scheldt estuary in 1978 compared to recent years. J Sea Res 42:275–290
20. Wen LS, Warnken KW, Santschi PH (2008) The role of organic carbon, iron, and aluminium oxyhydroxides as trace metal carriers: comparison between the Trinity River and the Trinity River Estuary (Galveston Bay, Texas). Mar Chem 112:20–37
21. Bibby RL, Webster-Brown JG (2005) Characterisation of urban catchment suspended particulate matter (Auckland region, New Zealand); a comparison with non-urban SPM. Sci Total Environ 343(1–3):177–197
22. Warren LA, Haack EA (2001) Biogeochemical controls on metal behavior in freshwater environments. Earth-Sci Rev 54(4):261–320
23. CIESM (2006) Fluxes of small and medium-size Mediterranean rivers: impact on coastal areas. Ciesm Workshop Monographs No. 30, Monaco
24. Haralambidou K, Sylaios G, Tsihrintzis VA (2010) Salt-wedge propagation in a Mediterranean micro-tidal river mouth. Estuarine Coastal Shelf Sci 90:174–184
25. Dassenakis M, Degaita A, Scoullos M (1995) Trace metals in sediments of a Mediterranean estuary affected by human activities (Acheloos river estuary, Greece). Sci Total Environ 168:19–31

26. Scoullos MJ, Pavlidou AS (2003) Determination of the lability characteristics of lead, cadmium and zinc in a polluted Mediterranean brackish-marine interface system. Water Air Soil Pollut 147(1–4):203–227
27. Scoullos MJ, Pavlidou AS (2000) Metal speciation studies in a brackish/marine interface system. Global Nest: Int J 2(3):255–264
28. Scoullos M, Dassenakis M, Zeri C (1996) Trace metal behavior during summer in a stratified Mediterranean system: The Louros estuary (Greece). Water Air Soil Pollut 88(3–4):269–295
29. Scoullos M, Zeri C (1993) The use of mineral magnetic measurements to study the transport and sedimentation of particles in the Gulf of Lions (NW Mediterranean). Oceanol Acta 16 (1):53–61
30. Scoullos M, Dassenakis M, Zeri C (1990) Study of the transport of metals in the estuary of Louros River during summer. In: Third hellenic symposium on oceanography and fisheries, Abst. Hellenic Centre for Marine Research (HCMR), Athens, pp 366–374
31. Scoullos M, Dassenakis M, Zeri C et al (1987) Chemical studies of main estuaries and coastal areas of Greece. Progress Report to DGXI, Project GEC-ENV-560 GR
32. Dassenakis M, Scoullos M, Gaitis A (1997) Trace metals transport and behaviour in the Mediterranean estuary of Acheloos River. Mar Pollut Bull 34(2):103–111
33. Kapsimalis V, Pavlakis P, Poulos SE, et al. (2005) Internal structure and evolution of the late quaternary sequence in a shallow embayment: The Amvrakikos Gulf, NW Greece. Mar Geol 222–223:399–418
34. Skoulikidis N (2009) The environmental state of rivers in the Balkans—A review within the DPSIR framework. Sci Total Environ 407:2501–2516
35. Kousouris T, Diapoulis A, Bertahas E, Gritzalis K (1989) Proceedings of the conference on environmental science and technology. Aegean University, Mytilini, pp. 300–309
36. Scoullos M, Dassenakis M, Gaitis A (1992) Distribution of nutrients in the Acheloos river mouth, Greece. Rapp Comm Int Mer Med 33:182
37. Skoulikidis N (2003) Hydrochemical character and spatiotemporal variations in a heavily modified river of western Greece. Environ Geol 43:814–824
38. Scoullos M, Maroulakou-Christodoulou M, Dassenakis M (1985) Preliminary results on the nutrient distributions in the Patraikos Gulf and the Acheloos Estuary. Rapp Comm Int Mer Medit 297:51–52
39. Anonymous (1992) The Greek river dilemma. Mar Pollut Bull 24(5):225
40. Close DH (1998) Environmental NGOs in Greece: the Acheloos campaign as a case study of their influence. Environ Polit 7(2):55–77
41. Scoullos M (1996) Environmental impacts of the Acheloos river diversion. Proceeding of the 15th congress of the international association of bridge and structural engineering, Copenhagen, pp 61–77
42. Mackereth FGH (1969) A short core sampler for sub aqueous deposits. Limnol Oceanogr 14:145
43. Riley JP, Taylor D (1968) Chelating resins for the concentration of trace elements from sea water and their analytical use in conjunction with atomic absorption spectrometry. Anal Chim Acta 40:479–485
44. Scoullos M, Dassenakis M (1984) Proceedings of the first hellenic symposium on oceanography and fisheries pp 302–309 (in Greek)
45. Agemian H, Chau ASY (1976) Evaluation of extraction techniques for the determination of metals in aquatic sediments. Analyst 101:761–767
46. Scoullos MJ, Oldfield F (1986) Trace metal and magnetic studies of sediments in Greek estuaries and enclosed gulfs. Mar Chem 18:249–268
47. Salomons W, Förstner U (1984) Metals in the hydrocycle. Springer–Verlag, Berlin
48. Kersten M, Smedes F (2002) Normalization procedures for sediment contaminants in spatial and temporal trend monitoring. J Environ Monit 4:109–115
49. Gaudette HE, Flight WR, Toner L, Folger DW (1974) An inexpensive method for the determination of organic carbon in recent sediments. J Sediment Petrol 44:249–253

50. Scoullos M, Botsou F, Zeri C (2014) Linking environmental magnetism to geochemical studies and management of trace metals. Examples from fluvial, estuarine and marine systems. Minerals 4:716–745
51. Viers J, Dupré B, Gaillardet J (2009) Chemical composition of suspended sediments in World Rivers: new insights from a new database. Sci Total Environ 407:853–628
52. Balls PW (1989) The partition of trace metals between dissolved and particulate phases in European coastal waters: a compilation of field data and comparison with laboratory studies. Neth J Sea Res 23(1):7–14
53. Rondeau B, Cossa D, Gagnon P, et al. (2005) Hydrological and biogeochemical dynamics of the minor and trace elements in the St. Lawrence River. Appl Geochem 20:1391–1408
54. Sholkovitz ER, Boyle EA, Price NB (1978) The removal of dissolved humic acids and iron during estuarine mixing. Earth Planet Sci Lett 40:130–136
55. Laslett RE, Balls PW (1995) The behaviour of disolved Mn, Ni, and Zn in the forth, an industrialized, partly mixed estuary. Mar Chem 48:311–328
56. Santos-Echeandía J, Prego R, Cobelo-García A, Millward GE (2009) Porewater geochemistry in a Galician Ria (NW Iberian Peninsula): Implications for benthic fluxes of dissolved trace elements (Co, Cu, Ni, Pb, V, Zn). Mar Chem 117(1–4):77–87
57. Benoit G, Oktay-Marshall SD, Cantu A, Hood EM, Coleman CH, Corapsioglu MO, Santschi PH (1994) Partitioning of Cu, Pb, Ag, Zn, Fe, Al and Mn between filter-retained particles, colloids, and solution in six Texas estuaries. Mar Chem 45:307–336
58. Turner A, Millward GE, Bale AJ, Morris AW (1993) Application of the KD concept to the study of trace metal removal and desorption during estuarine mixing. Estuarine Coastal Shelf Sci 36:1–13
59. Benoit G, Rozan TF (1999) The influence of size distribution on the particle concentration effect and trace metal partitioning in rivers. Geochim Cosmopolitica Acta 63:113–127
60. Sholkovitz ER (1978) The flocculation of dissolved Fe, Mn, Al, Cu, Ni, Co and Cd during estuarine mixing. Earth Planet Sci Lett 41(1):77–86
61. Rudnick RL, Gao S (2003) Composition of the continental crust In: Rudnick RL (ed) Treatise on geochemistry, vol 3. Elsevier, Oxford, pp 1–64
62. Bacon JR, Davidson CM (2008) Is there a future for sequential chemical extraction? Analyst 133:25–46
63. Shannon RD, White JR (1991) The selectivity of a sequential extraction procedure for the determination of iron oxyhydroxides and iron sulfides in lake sediments. Biogeochemistry 14:193–208
64. Peltier E, Dahl AL, Gaillard JF (2005) Metal speciation in anoxic sediments: when sulfides can be construed as oxides. Environ Sci Technol 39:311–316